Preparations, Characterizations and Applications of Chitin Nanofiber and Its Derivatives

January, 2017

Fantahun Aklog Yihun

Department of Chemistry and Biotechnology

Graduate School of Engineering

Tottori University

Contents

List of figures

List of tables

General introduction

Chitin, the second most abundant carbohydrate polymer on earth next to that of cellulose, is an ideal candidates for various applications due to its remarkable properties such as abundance, biodegradability, biocompatibility, antibacterial activity, and high mechanical performance. Its annual biosynthesis rate is estimated to 100 billion tons.[1] Despite these intrinsic advantages, large amount of chitin is still thrown away as industrial waste mainly because of its strong inter and intra molecular hydrogen bonds, which make it insoluble in water and common organic solvents. Structurally chitin is a linear polysaccharide composed of β-(1, 4)-linked 2-acetamido-2-deoxy-D-glucose units, though to some extent N-acetyl glucosamine units are present in the natural system.[2] Chitin has a similarity to cellulose both in chemical structure and in biological function as a structural polysaccharide and can be defined as a cellulose derivative with an acetamido group at C-2 position (Figure 1b). Cellulose strengths the cell wall of plants whereas chitin contributes to the mechanical strength of fungal cell walls and the exoskeletons of arthropods.[3] Chitin is predominantly present as a fibrillar crystalline material. Based on infrared spectroscopy and x-ray diffraction data, native chitin can occur in one of the three crystalline forms:α , β, or γ depending on its origin.[4] α-chitin is the most abundant form, which exist in crabs, lobsters, krill and shrimps shells, insect cuticle, and fungal and yeast cells walls.[5] On the other hand the main sources of β –chitin are squid pens and tubeworms,[6,7] and the molecular chains are arranged in a parallel fashion, while γ-chitin is the form in which the molecules are arranged in both parallel and antiparallel manner.

Commercially pure chitin can be extracted from crab and shrimp shells by chemical treatment. Treatment of these biowaste using hazardous chemicals involves alkalis (usually 4 wt. % NaOH) for deproteinization and strong acids (4 wt. % HCl) for demineralization, making

this process ecologically aggressive, economically costly and is a source of pollution.[5,8] In addition to the cost of the chemicals use for deproteinization and demineralization, the extraction cost of chitin by the chemical method can be increased since more chemicals are needed for neutralization and detoxification of the discharged waste water. Another disadvantage of chitin extraction by the chemical method is that the valuable protein components can no longer be used as animal feed. Therefore, it is crucial to design a mechanism for the preparation of materials from the chitin biomass with little or without chemical treatments for those applications that do not require the pure form of chitin. For pure chitin extraction, a biological method is becoming an alternative route to alleviate the drawbacks of chemical method. However, the biological method of chitin extraction has a problem of complete removal of the minerals and proteins from chitin biomass in addition to its slowness.

As a result of its extraordinary properties, chitin has many applications in different areas such as wound healing, anti-microbial activity, tissue engineering, cosmetics, food, fertilizer, textiles and drug delivery, pulp and paper industries etc.[9,10]

Chitosan (Figure 1c) is a linear polyaminosaccharide derived by the deacetylation of chitin. Unlike chitin, chitosan is less common in nature, but is present as a cell wall component of filamentous fungi, where chitosan biosynthesis is through deacetylation of chitin.[11] Chitosan becomes soluble in acidic aqueous solutions and behaves as a cationic polyelectrolyte due to the protonation of amine groups in the presence of H^+ ions.[12] Commercially, chitosan can be obtained from shrimp or crab shell chitin in which the N-acetyl glucosamine units get converted into glucosamine units by deacetylation using 40-50 wt. % NaOH or KOH aqueous solution.[13] Chitosan degree of deacetylation (DDA) is an important parameter that determines the physicochemical and biological properties of chitosan such as crystallinity, hydrophilicity, degradation and cell response.[14,15] It was reported that prolonged degradation times and

enhanced cell adhesion can be achieved using chitosan with a DDA close to 0 % or 100 % while chitosan with intermediate DDAs exhibit rapid degradation rates, but at the cost of limited cell adhesion.[14] In another study it was also described that chitosan membranes between 65 and 80 % DDA elicited marked inflammatory reactions that subsided in time with degradation of the films, granulation tissue formation, and osteogenesis while membranes made of 94 % DDA chitosan showed minimal degradation, mild inflammation and minimal osteogenesis.[16] Chitosan with desired degree of deacetylation can be obtained by controlling the alkali concentration and the deacetylation reaction time and temperature. Another important parameter which has its own influence on the properties and functions of chitosan is molecular weight. Many researchers explained the effect of molecular weight of chitosan on its antimicrobial and biological activities. It was reported that chitosan with lower molecular weight showed superior biological activities compared to high molecular weight.[17]

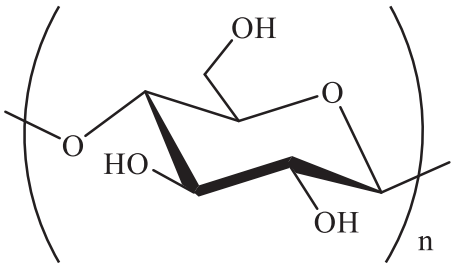

(a) Cellulose

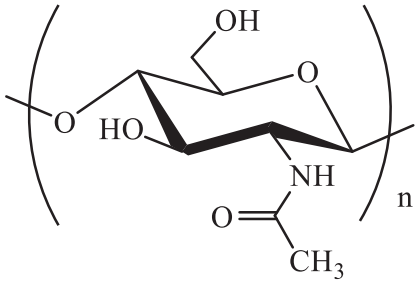

(b) Chitin

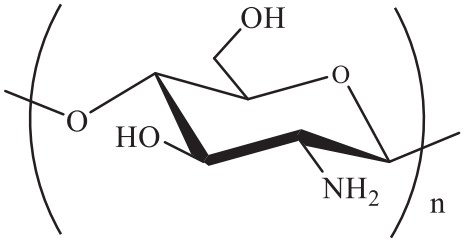

(c) Chitosan

Figure 1.Chemical structure of (a) cellulose, (b) chitin, and (c) chitosan.

Nanofibers are usually defined as fibers with diameters less than 100 nm. They have several advantages over the bulk materials, such as very large aspect ratio, higher mechanical, electrical, and optical properties, and greater chemical reactivity. These extraordinary properties make the nanofibers to be optimal candidates for many applications such as water and air filtration, protective and lightweight clothing, as scaffolds in tissue engineering, wound dressing, drug delivery, as nanofillers in the field of polymer nanocomposites etc.[18-23] In recent years much attention has been given in the productions, characterizations and applications of nanofibers from biopolymer sources due to their superior qualities over other nanofibers in terms of their biodegradability, biocompatibility, low toxicity, renewability and sustainability.

Based on the points mentioned above, the author used the biopolymer chitin and its derivatives as raw materials for nanofibers synthesis. Moreover, an environmentally friendly simple mechanical treatments were employed for nanofibers preparation. The thus obtained nanofibers were characterized in terms of their morphology, transparency, viscosity, chemical and crystalline structures, and thermo-mechanical properties. The author investigated the fertilizer application of protein/$CaCO_3$/chitin nanofibers complex for plant growth. Finally, the author modified the surface of chitin to increase nanofibrillation and nanofibers' reinforcement effect in the field of polymer nanocomposites.

Briefly, in chapter 1, the effect of grinder pre-treatment on the fibrillation of α-chitin into nanofibers using high pressure water jet (HPWJ) system was described. The nanofibers' morphology, viscosity and light transmittance measurement results clearly demonstrated that pre-grinder treatment has played a great roll for the nanofibrillation of α-chitin at lower passes of subsequent HPWJ treatments. The chemical and crystalline structure of the original α-chitin remained unchanged with the pre-grinder and subsequent HPWJ mechanical treatments.

Chapter 2 represents the preparation of chitosan nanofibers from completely deacetylated chitosan powder by a downsizing process. Chitosan nanofibers from 100 % degree of deacetylated (DDA) chitosan powder were successfully prepared by high pressure water jet (HPWJ) system. The field emission scanning electron microscope (FE-SEM) images indicated that nanofibrillation of chitosan was completed at around 10 passes of HPWJ treatment, but further mechanical treatments did not show any significant change on nanofibers' thickness. The viscosity and transparency of the nanofibers slurry also revealed that high morphological change was ensued at around 10 passes of HPWJ treatment. Relative crystallinity of chitosan nanofibers gradually decreased as the number of passes increased since HPWJ treatment damaged the crystalline region of chitosan nanofibers. The molecular weights of the nanofibers steeply decreased due to the depolymerization of chitosan by mechanical disintegration. The mechanical properties of chitosan nanofiber sheets such as young's modulus and tensile strength were significantly enhanced with increasing number of treatments by HPWJ system, but above 30 cycles treatment the tensile strength was deteriorated.

In chapter 3, chitin nanofibers were prepared by surface esterification of α-chitin with maleic anhydride and mechanical treatment. A solventless reaction procedure was employed to modify the surface of chitin with maleic anhydride. This made the esterification reaction procedure simple and environmentally friendly. Only two cycles grinder treatment were used for the disintegration of chitin into uniform 10-nm average thickness nanofibers. The maleate groups grafted on the surface of chitin remarkably increased nanofibrillation and water dispersibility of the nanofibers as a result of electrostatic repulsion between carboxylate anions. Hence the nanofibers preparation method was extremely cost effective. XRD data revealed that esterification was proceeded on the surface and did not affect the relative crystallinity. Both the basic water dispersion and cast film of the esterified chitin nanofibers were highly transparent

compared with the unmodified chitin nanofibers obtained through the same mechanical treatment.

Chapter 4 describes the preparation of protein/$CaCO_3$/chitin nanofiber complex from crab shells by a simple mechanical treatment and its effect on plant growth. The crab shells were directly crashed and disintegrated into nanofibers using pre-grinder and subsequent high pressure water jet (HPWJ) mechanical treatments. The preparation process did not involve chemical treatments, such as removal of protein and calcium carbonate with sodium hydroxide and hydrochloric acid, respectively. Thus, it was economically and environmentally friendly. Results from the nanofibers' morphology, transparency and viscosity showed that the shells were mostly disintegrated into nanofibers at around five cycles of the HPWJ treatment. FT-IR data confirmed that the chemical structure of the nanofibers was maintained even after extensive mechanical treatments. The nanofiber complex has shown improvement on the growth of tomatoes in a hydroponics system, suggesting the mechanical treatments efficiently released minerals into the system.

Chapter 1

Effect of grinder pretreatment for easy disintegration of chitin into nanofiber

1.1. Introduction

Chitin is the most widespread amino polysaccharide in nature and is estimated annually to be produced almost as much as cellulose. It is abundantly present in the exoskeletons of crustaceans such as crabs and shrimps. These exoskeletons have a hierarchal organization consisting of the α-chitin nanofibers, several proteins, and minerals.[24,25] The original chitin in crab shells have an anti-parallel molecular chain alignment forming nanofibers connected by inter and intra molecular hydrogen bonds.[26] These microfibers consist of nanofibers having diameter about 2-5 nm, and length of about 300 nm embedded by protein matrices.[24,25]

Because of their extremely small size and large surface area to volume ratio, nanofibers are attracting much attention in various fields. Chitin nanofibers have additional qualities owing to their biopolymer source of chitin macromolecule. As a result of their great potential applications in the rapidly growing field of bionanotechnology, various methods have been employed for the extraction of chitin nanofibers from their source, including acid hydrolysis,[27] TEMPO mediated oxidation,[28] an ultrasonic technique,[29] and an electrospinning method.[30] However, the nanofibers obtained through these methods were different from the native chitin nanofibers in terms of chemical structure, width, aspect ratio, crystalline structure, and homogeneity.[26] The effectiveness of chitin nanofibers for different application is strongly affected by their extraction method. Recently, chitin nanofibers with a uniform width of 10 nm

were successfully isolated from outer shells of crabs,[31] prawns,[32] and from the cell walls of mushrooms[33] using a simple grinder machine in acidic solution. More recently, chitin nanofibers from dry chitin powder of crab shells were prepared using a new atomizing system called high pressure water jet (HPWJ) system, and the advantages of this system for chitin nanofibers preparation in acidic condition were described as (1) The amount of chitin slurry formation can be easily arranged to a large extent from 2 to 840 l/h by changing the scale of the HPWJ equipment from small to large. (2) In principle, the system can produce the same nanofibers independent of the scale of the equipment, as long as the ejection pressure of sample from the small nozzle is constant. (3) This process is free from contamination.[34] Thus, the HPWJ system has many advantages, such as being environmentally friendly, preserving both the crystalline and chemical structure of the native chitin nanofibers, making nanofibers that are small in width with a high aspect ratio, and allowing production of thinner and properly nanofibrillated chitin fibers. However, the sample must be passed through the system at least 10 times.[35] As a consequence of long time needed for the homogenization of the chitin nanofibers, the system also required a lot of energy, which make the large scale production of chitin nanofibers using HPWJ system economically infeasible. Since HPWJ system has many strong sides compared with other methods, it is indispensable to find a solution for its problems and make it a promising method of chitin nanofibers production in large scales.

In this study, the author applied grinder apparatus for pre-treatment of chitin. The effect of grinder pre-treatment on the preparation of chitin nanofibers from crab shells dry chitin powder by HPWJ system was studied. Certainly crushed chitin by grinder could be effectively disintegrated into nanofiber by subsequent HPWJ treatment, which reduces number of cycles of HPWJ treatments. The obtained nanofibers were characterized based on the morphology, transparency, viscosity, and chemical and crystalline structures.

1.2. Experimental

1.2.1. Materials

α-chitin powder from crab shell with a 6.4% degree of deacetylation (DDA) was purchased from Koyo Chemical Industry and used without further purification. Acetic acid was purchased from Kanto chemical and used as received.

1.2.2. Pre-grinder and subsequent high pressure water jet (HPWJ) treatments of chitin

Dry chitin powder was dispersed in water at 1 wt. %. Acetic acid with 0.5 wt. % was added to facilitate mechanical disintegration. After one hour stirring, the inhomogeneous water dispersion was pretreated by a grinder (MKCA6-3; Masuko Sangyo) at 1500 rpm for zero (G-0), one (G-1), and two times (G-2). After grinder treatment, each sample (G-0, 1, and 2) were stirred under vacuum for one hour to remove tiny air bubbles. Finally, the dispersion of each sample was mechanically treated for 1, 5, 10 and 30 cycles by the HPWJ system (Star Burst Mini, HJP-25001S, Sugino Machine) equipped with a ball collision chamber. The slurry was ejected from a small nozzle with a diameter of 100 μm under high pressure (245 MPa) and collided with a ceramic ball with a diameter of 12.7 mm.

1.2.3. Characterization

1.2.3.1. Analysis of morphological changes

The morphological changes of α-chitin due to mechanical treatments were characterized using field emission scanning electron microscopic (FE-SEM). To do so the prepared nanofiber suspensions were diluted with ethanol and dried in an oven. The dried samples were coated with

an approximately 2 nm layer of platinum using an ion sputter coater and were observed by FE-SEM (JSM-6700F; JEOL, Ltd) operating at 2.0 kV.

1.2.3.2. Elucidation of chemical and crystalline structures of chitin nanofibers

The chemical structure of the nanofibers were determined by the fourier transform infrared (FT-IR) spectroscopy. The spectra of the samples were recorded with an FT-IR spectrophotometer (Spectrum 65, Perkin-Elmer Japan) equipped with an attenuated total reflection (ATR) attachment.

The crystalline structure of the obtained nanofibers were determined using a wide angle x-ray diffraction technique. The x-ray diffraction profiles were obtained with Ni-filtered CuKα from an x-ray generator (Ultima IV, Rigaku) operating at 40 kV and 30 mA. The diffraction profiles were detected using x-ray goniometer scanning from 5 to 60°. The crystallinity index (CI) of each sample was estimated using the equation:

$$\mathrm{CI}(\%) = \left(\frac{\mathrm{I_{110}-I_{am}}}{\mathrm{I_{110}}}\right) \mathrm{x100} \qquad (1)$$

Where I_{110} is the maximum intensity at approximately 19.1° of the 110 lattice diffraction and I_{am} is the minimum intensity of the amorphous diffraction at approximately 14.5°.[36]

1.2.3.3. Light transmittance and viscosity measurements

The light transmittances with 0.1 wt. % chitin nanofiber suspensions were measured using a UV–Vis spectrophotometer (V550; JASCO, Tokyo, Japan) in a wave length range of 200-800 nm. The viscosities of 1.0 wt. % chitin nanofiber slurries were measured by a Brookfield digital viscometer DV-E using the LV-3 spindle (Brookfield Engineering Laboratories, Middleboro, MA) at a temperature of 30 °C.

1.3. Results and discussion

1.3.1. SEM observation of chitin nanofibers

Figure 2 shows the morphological changes of chitin at different number of pre-grinder and HPWJ treatments in acidic solution. “G-x, H-y” represents number of mechanical treatments using pre-grinder and subsequent HPWJ system, respectively. Sample of G-0, H-0 indicates original chitin powder without any mechanical treatment. Fibrous chitin aggregate was observed on the surface. In G-0, H-1 sample, the aggregates of chitin fibers were slightly separated. Above 5 cycles of HPWJ treatment, chitin was considerably disintegrated into thinner fiber. With increasing the number of HPWJ treatments, chitin became thinner and fine nanofiber network was observed. Meanwhile with a single grinder treatment (G-1, H-0), the sample was roughly separated and consisted of micro and nanosized chitin fibers. Subsequent single HPWJ treatment (G-1, H-1) caused drastic change in chitin fiber morphology, comparing with change from G-0, H-0 to G-0, H-1. Most of micro sized chitin fibers were mechanically atomized into nanosized chitin fiber. Additional HPWJ treatment showed further changes in nanofiber structure. Structural changes of G-1 samples were almost the same as two cycles grinder pretreated samples. After two passes (G-2 H-0), mixture of nano and micron sized fibers were observed. Subsequent 1 pass HPWJ treatment (G-2, H-1) caused effective disintegration of the micro sized fibers into nanoscale. However, excessive HPWJ treatments did not change in nanofiber diameter. On the other hand, length of nanofibers was considerably decreased over 10 cycles of HPWJ treatment. This is due to the mechanical scission of fibers in length during the nanofibrillation process. Generally the grinder pretreatments strongly enhanced the nanofibrillation by subsequent single HPWJ treatment (compare G-0, H-1 to G-1/2, H-1).The pretreatment could transform the chitin powder into homogeneous submicron

fibers since thicker fibers cannot pass through the narrow clearance gap between pair of grinding stones, which is helpful for further disintegration by HPWJ treatment.

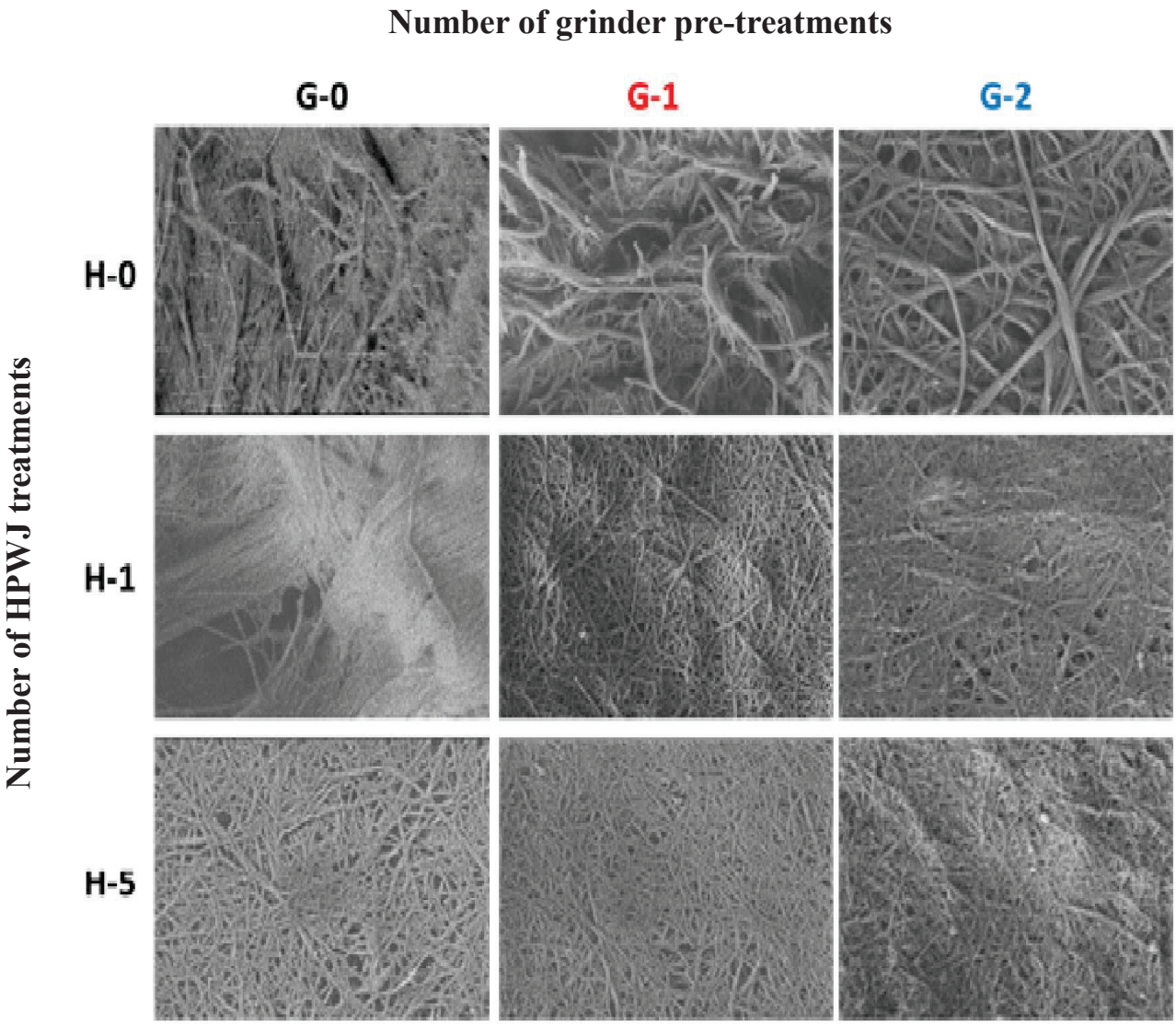

Figure 2. FE-SEM micrographs of chitin nanofibers after grinder pre-treatment and subsequent high pressure water jet treatment. Scale bars are 500 nm.

1.3.2. Chemical and crystalline structures of chitin nanofibers

The FT-IR spectra of the series of mechanically treated samples were collected in the wave number range of 500-4000 cm^{-1}. All the spectra of the samples were in excellent agreement with each other, and were the same as that of the original pure chitin powder. This indicates that the original chemical structure of chitin was maintained despite the powerful mechanical load provided by grinder and/or HPWJ system.

The crystalline structures of chitin fibers after mechanical treatment were examined by wide angle x- ray diffraction. All the samples showed the same pattern and major reflections were observed at approximately $2\theta = 9.1^{o}$ and 19.1^{o}. These peaks correspond to 020 and 110 planes of crystalline unit cells, respectively.[36] Minor reflections were also detected at around $2\theta = 20.5^{o}$, 23.1^{o}, and 26.1^{o}. These diffraction peaks are the typical antiparallel crystal patterns of α chitin.[37] This showed that the crystalline structure of the original chitin fibers was unchanged during the nanofibrillation process by the pre-grinder and subsequent HPWJ mechanical treatments. Table 1 shows the relative crystallinity indices of chitin fibers obtained from those x-ray diffraction profiles. Relative crystallinity of original chitin was 88.0 % (G-0, H-0). After grinder pretreatment (G-1, H-0 and G-2, H-0), crystallinity of the three samples were nearly constant. Degree of crystallinity was remained the same even after HPWJ treatments. This result confirmed that the grinder pretreatment and/or HPWJ treatments did not distort the crystalline structure of the original chitin.

Table 1. Degree of relative crystallinities of chitin nanofibers after pre-grinder and subsequent HPWJ treatments.

Number of mechanical treatment	Relative crystallinity (%)				
	H-0	H-1	H-5	H-10	H-30
G-0	88.0	85.8	89.6	84.4	84.9
G-1	88.3	86.3	87.8	85.6	86.3
G-2	88.8	87.3	89.8	87.7	86.0

1.3.3. Transparency and viscosity of chitin nanofiber suspensions

Figure 3 represents the regular light transmittance of mechanically treated chitin dispersion with 0.1 wt. % concentration at 600 nm wave length. The transmittance of the dispersion provides information about morphological change in nanofibers. Fiber thickness strongly affects the transparency of the dispersion since thicker fiber caused light scattering. As the number of passes of the HPWJ treatment increased, light transmittance of all pretreated samples (G-0, G-1, and G-2) increased. Transmittance of G-2 sample was slightly higher than that of G-1 sample, indicating thinner nanofiber. Both G-1, H-0 and G-2, H-0 mechanically treated samples transmittance steeply increased after a single HPWJ treatment (46.4 and 52.6 %, respectively), and gradually increased up to 30 passes. This indicated that chitin fiber thickness was significantly decreased after a single HPWJ treatment, and gradually reduced over 1-30 passes. On the other hand the light transmittance of G-0 sample was considerably lower than that of G-1 and G2 samples in each number of passes. Especially, after single HPWJ treatment (G-0, H-1) little increase in transmittance was observed (6.2 %), which is considerably lower

than that of pretreated samples. This suggests that grinder pretreatment provides homogeneous chitin dispersion in water, and enables higher light transparent even with single HPWJ treatment. For instance, the light transmittance of G-1, H-1 slurry (46.4 %) has almost the same value to that of G-0, H-5 slurry (47.1 %). The trend agreed well with the result from SEM micrographs (Figure 2).Therefore, from this result it can be concluded that grinder pretreatment accelerated the efficiency of HPWJ mechanical treatment for easy nanofiber preparation.

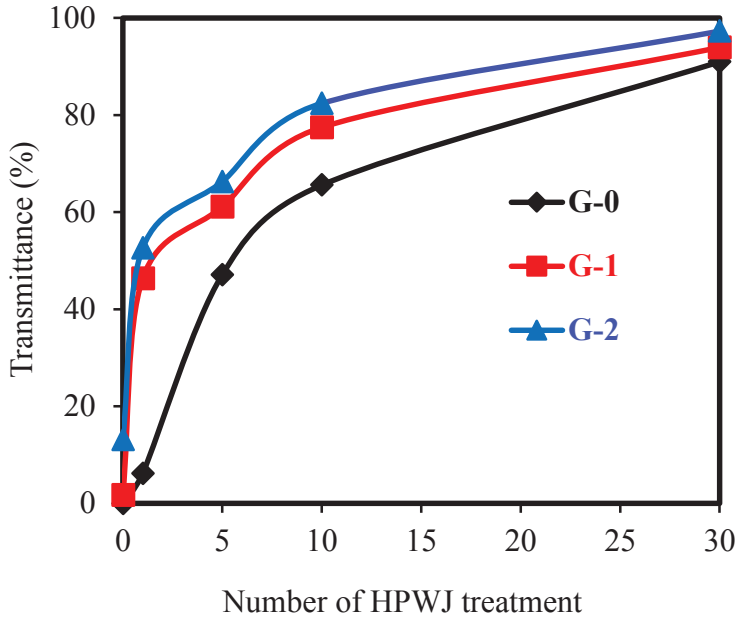

Figure 3. Regular light transmittances of 0.1 wt. % chitin suspension after grinder pretreatment as a function of the number of cycles of subsequent HPWJ treatments.

Figure 4 shows the viscosities of grinder pretreated chitin fiber slurries with 1.0 wt. % concentration as a function of number of treatments by the HPWJ system. Viscosity is also strongly associated to the morphology of the chitin nanofibers. Thinner and longer nanofibers have higher viscosity, due to the increase in interfibrillar interaction of nanofibers. The viscosities of G-1 and G-2 samples linearly increased up to 5 passes of HPWJ treatment. This indicated that the chitin fibers of these samples became thinner up to 5 passes. Interestingly, further HPWJ treatments caused a steeply decreased in viscosity of nanofibers. This suggests

that excessive HPWJ treatment decreased the length of fibers, which reduced viscosity by freeing the nanofibers from entanglements. Although G-1 and G-2 samples followed the same trend, the viscosities of G-2 series were greater than the G-1 series up to 5 passes. This showed that G-2 samples were thinner and longer than G-1 samples up to 5 passes of HPWJ treatments. On the contrary, the non-treated sample (G-0) showed considerably lower viscosity than pretreated samples with up to 10 passes of HPWJ treatments. Moreover, viscosity of the G-0, H-1 sample was only 107 cP, considerably lower than that of the G-1, H-1 and G-2, H-1 samples (3723 cP and 4730 cP, respectively). Thus, viscosity measurements clearly revealed the effect of grinder pretreatment for nanofiber production. Even a single grinder pretreatment was effective in increasing the ease of chitin nanofiber preparation. As a result, viscosity of the G-1, H-1 slurry (3723 cP) was almost same with that of the G-0, H-5 slurry (4017 cP).

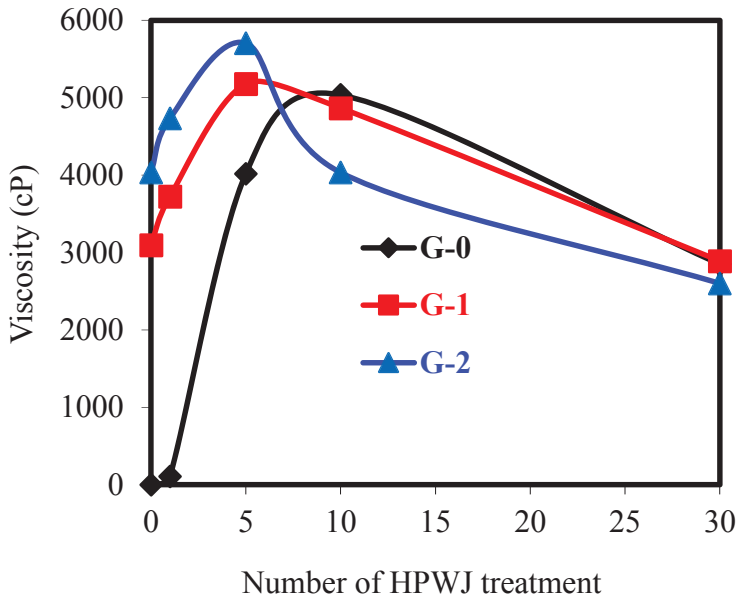

Figure 4. Viscosities of chitin suspension after grinder pretreatment as a function of the number of cycles of subsequent HPWJ treatment.

1.4. Conclusion

Chitin nanofibers were prepared from dry chitin powder by a series of mechanical treatments. Since commercial chitin consists of aggregated nanofibers, chitin powders were converted into thinner fibers by mechanical load. Morphology, chemical structure, relative crystallinity, transparency, and viscosity of obtained chitin nanofibers were characterized. Data series showed that even a single grinder pretreatment was very effective in improving subsequent HPWJ treatment for nanofiber production. Although the HPWJ system generates a strong collision force, a considerable number of HPWJ treatments were required for complete nanofibrillation. Only a single grinder pretreatment could reduce the number of HPWJ treatments needed, which would decrease the production cost of chitin nanofiber. In conclusion, the G-1, H-1 sample corresponded to the G-0, H-5 sample in transparency and viscosity of nanofibers. Thus, this easy procedure will enhance the commercial application of chitin nanofibers.

Chapter 2

Preparation of chitosan nanofibers from completely deacetylated chitosan powder by a downsizing process

2.1. Introduction

Chitosan has a weak cationic linear polysaccharide structure consisting of β-(1-4)-linked 2-amino-2-deoxy-D-glucopyranose repeating units. By virtue of its biocompatibility and biodegradability, as well as its cell binding, wound healing, antibacterial, and antifungal properties, chitosan has great potential in food, cosmetic, biomedical, and pharmaceutical applications.[38-42] Due to their unique morphology, nanofibers are quite different from microsized fibers in their dimensional, optical, and mechanical properties. Therefore, the preparation of chitosan nanofibers is also an important subject. Electrospinning is the most popular way to produce artificial nanofibers from a wide range of polymer solutions using interactions between fluid dynamics, electrically charged surfaces, and electrically charged liquids.[43-45] However, it is difficult to electrospin chitosan, since the cationic charge increases the excessive surface tension of the solution,[46] which resulted in a high electrical force demand for nanofiber production. Therefore, other synthetic polymer is usually added with chitosan to improve its electrospinnability.[47-50]

Chitin nanofibers from a commercial chitin powder made from crab shell were successfully prepared by a simple grinder treatment in acidic environment.[31] Since the chitin powder is made up of regularly structured chitin nanofiber aggregates, it was disintegrated into nanofibers by mechanical treatment.[51] The chitin nanofibers obtained have a highly uniform

network morphology. It was reported that chitin nanofibers have a powerful biological activities. For instance, they have anti-inflammatory actions via the suppression of NF-$_k$B and MCP-1 activations and suppress fibrosis in an acute ulcerative colitis mouse model.[52,54] Furthermore, the application of chitin nanofibers to skin improved the epithelial granular layer, increased granular density, and reduced production of TGF-β.[54,55]

In recent years, by applying the downsizing technique, chitosan nanofibers were also easily prepared from commercially available chitosan with a 78% deacetylation degree.[56] These nanofibers were characterized in detail. The author expected that chitosan nanofibers also have several biological activities that would be useful for food, cosmetic, biomedical, and pharmaceutical applications. To distinguish between chitin and chitosan nanofibers, chitosan nanofibers must be strictly deacetylated to know the biological properties of chitosan nanofibers. In this study, the author reported the preparation of chitosan nanofibers with a 100 % deacetylation degree by using a high pressure water jet system and these nanofibers were characterized in terms of their morphology, transparency, viscosity, average molecular weight and mechanical properties.

2.2. Experimental

2.2.1. Materials

Chitosan powder with a 100 % degree of deacetylation (DDA) (Koyo Chitosan DAC100) was purchased from Koyo Chemical Industry and used without further purification.

2.2.2. Preparation of chitosan nanofibers

Chitosan powder was dispersed in deionized water at a 1 wt. % concentration. The dispersion was roughly crushed with a grinder (MKCA6-3; Masuko Sanyo) at 1500 rpm and was stirred overnight at room temperature. Then the crushed chitosan dispersion was passed through a high pressure water jet system (Star Burst Mini, HJP-25001S, Sugino Machine) equipped with a ball collision chamber. The slurry was ejected from a small nozzle with a diameter of 100 μm under high pressure of 200 MPa and collided with a ceramic ball with a diameter of 12.7 mm. The mechanical treatment was repeated for 1, 3, 5, 10, 30, and 50 cycles.

2.2.3. Preparation of chitosan nanofiber sheets

Chitosan nanofibers were diluted with deionized water by 0.1 wt. % of fiber content. After removal of dissolved gases under vacuum, the suspensions were vacuum filtered with a membrane filter. The obtained chitosan nanofiber sheets were dried by hot pressing at 100 ˚C for 30 min. The dried sheets were cut into 5 cm squares with an approximate thickness and weight of 65 μm and 100 mg, respectively.

2.2.4. Characterization

2.2.4.1. Chitosan nanofibers morphological observation

For field emission scanning electron microscopic (FE-SEM) observation, the prepared chitosan nanofiber suspensions were diluted with ethanol and dried in an oven. The dried samples were coated with an approximately 2 nm layer of platinum using an ion sputter coater and were observed by FE-SEM (JSM-6700F; JEOL, Ltd) operating at 2.0 kV.

2.2.4.2. Determination of chemical and crystalline structures of chitosan nanofibers

Infrared spectra of the samples were recorded with an FT-IR spectrophotometer (Spectrum 65, Perkin-Elmer Japan) equipped with an ATR attachment. The x-ray diffraction profiles were obtained with Ni-filtered CuKα from an x-ray generator (Ultima IV, Rigaku) operating at 40 kV and 30 mA. The diffraction profiles were detected using x-ray goniometer scanning from 5 to 40°. The crystallinity index (CI) of each sample was estimated using equation (1) i. e, $CI(\%) = \left(\frac{I_{110}-I_{am}}{I_{110}}\right) x100$, where I_{110} is the maximum intensity at approximately 20° of the 110 lattice diffraction and Iam is the minimum intensity of the amorphous diffraction at approximately 15.5°.[57]

2.2.4.3. Light transmittance and viscosity measurements

The light transmittances with 0.1wt. % chitosan nanofiber suspensions were measured using a UV–Vis spectrophotometer (V550; JASCO, Tokyo, Japan). The viscosities of 1.0 wt. % chitosan nanofiber slurries were measured by a Brookfield digital viscometer DV-E using the LV-4 spindle (Brookfield Engineering Laboratories, Middleboro, MA).

2.2.4.4. Molecular weight determination

The molecular weights of dried chitosan nanofibers were measured by the viscosity method with an Ubbelohde capillary type viscometer (NO W-1103, Kusano Science, Tokyo, Japan) in 0.2 M acetic acid and 0.1 M sodium acetate aqueous solution in concentration ranges of 5.8–12.5 g/L at 30 °C. The specific viscosities were calculated from the equation:

$$\eta_{sp} = \left(\frac{t}{t_o} - 1\right) \quad (2)$$

The parameters t and t_o were the flow times of the solvent with and without the samples, respectively. Three flow time measurements were done for each solution. The flow time data

were used to calculate the specific viscosity [η_{sp}] and then the intrinsic viscosities [η] were determined using the equation:

$$[\eta] = \lim_{C \to 0} \frac{\eta_{sp}}{c} \quad (3)$$

Where c, is the polymer concentration, and the intrinsic viscosity of each sample was estimated by extrapolation of $\frac{\eta_{sp}}{c}$ to zero concentration.

Finally, with the intrinsic viscosity results, the Mark–Houwink-Sakurada equation was used to calculate the viscosity average molecular weight (Mv) of chitosan nanofibers:

$$[\eta] = k(M_v)^{\alpha} \quad (4)$$

Here K (16.80×10^{-3}) and α (0.81) are empirical constants valid for a specific polymer solvent system at a given temperature.[58]

2.2.4.5. Tensile testing measurement

The young's modulus and the tensile strength of the chitosan nanofiber sheets were measured using a universal testing instrument (AG-X, Shimadzu, and Tokyo, Japan) for samples 5 cm in length and 1 cm in width. For each sample, five specimens were tested.

2.3. Results and discussion

2.3.1. SEM micrographs of chitosan nanofibers

Figure 5 shows the morphological changes of chitosan with 100 % DDA as a result of the high pressure water jet treatment with 0, 1, 5, 10, 30, and 50 passes in water. In Figure 5a, a fibrous structure can be seen, indicating that chitosan powder was roughly crushed by 2 cycles

grinder pre-treatment. After one pass of the high pressure water jet treatment, the chitosan was reduced to micro and nanosize fibers (Figure 5b). After five passes, the fiber thickness had decreased further, meaning the microfibers had become fibrillated (Figure 5c). However, the fiber morphology was heterogeneous and submicron sized fibers remained. After 10 cycles, most of the chitosan had been reduced to homogeneous nanofibers measuring tens of nanometers and showed a fine network structure (Figure 5d). On the other hand, further mechanical treatment did not show a significant change in nanofiber structure. This result is similar to that of 78 % DDA chitosan. Thus, mechanical treatment effectively disintegrated 100% of the DDA chitosan powder. Although a strong basic condition is required for the complete deacetylation of chitin, the nanofiber aggregate structure of chitin powder was maintained after the deacetylation reaction, allowing fully deacetylated chitosan nanofibers to be obtained.

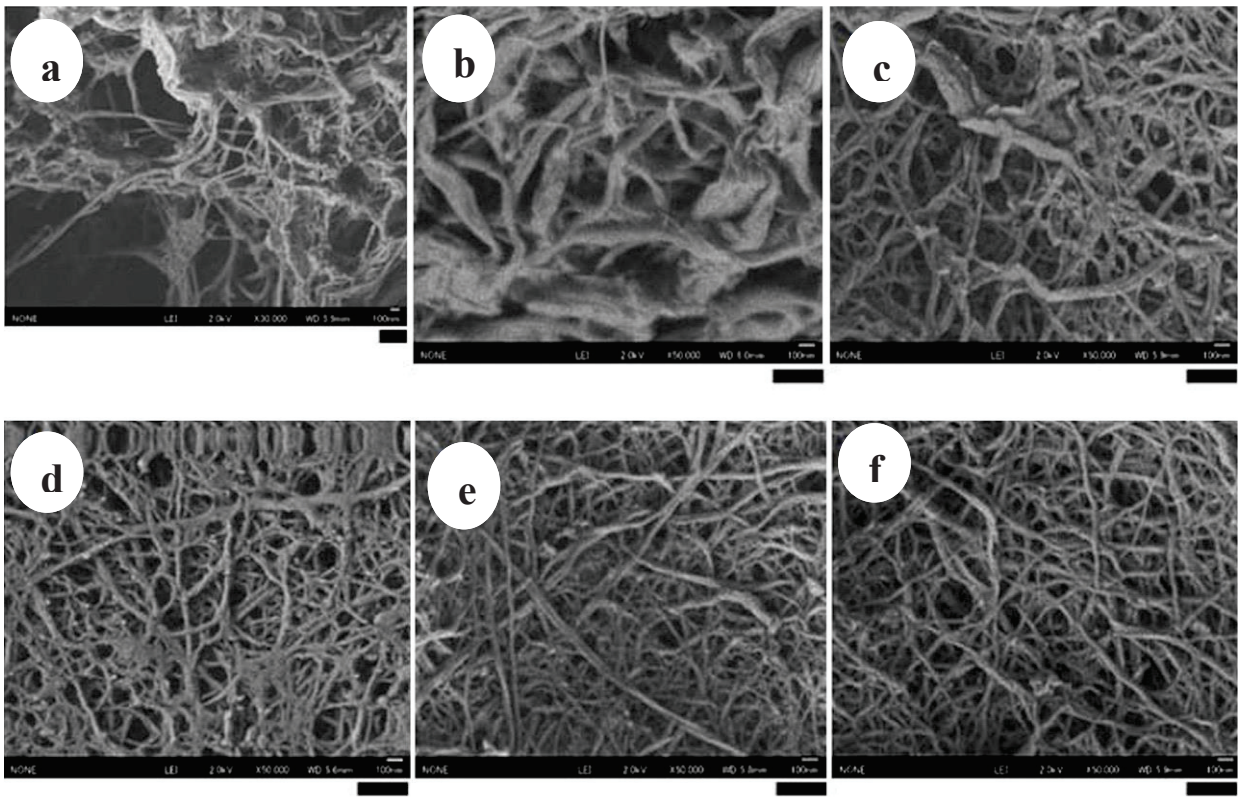

Figure 5. FE-SEM micrographs of chitosan fibers after (a) 0, (b) 1, (c) 5, (d) 10, (e) 30, and (f) 50 passes through the high pressure water jet system. Scale bars are 300 nm. Reproduced with permission from *International Journal of Biological Macromolecules* **2015**, *72*, 1191–1195. Copyright 2014, Elsevier.

2.3.2. Chemical and crystalline structures of chitosan nanofibers

The FT-IR spectra of chitosan fibers processed after 0, 1, 5, 10, 30, and 50 passes were used to evaluate their chemical structure. Each sample exhibited a number of absorption peaks. The broad band at around 3363 cm^{-1} is related to the stretching vibration of O-H overlapped with N-H stretching vibration band. The peak at around 2877 cm^{-1} is due to the C-H stretching vibration attributed to the pyranose ring. The absorption band at 1591 cm^{-1} could be assigned to the N-H bending vibration of the amine group. Peaks at around 1422 cm^{-1} and 1376 cm^{-1} are allocated to the bending vibration of CH_2 in CH_2OH group and C-H in the pyranose ring, respectively. The peak at 1151 cm^{-1} is due to the antisymmetric stretching vibration of C-O-C bridge. Absorption bands at around 1028 cm^{-1} and 1078 cm^{-1} are related to the C-O stretching of primary and secondary alcohols in the chitosan structure, respectively. Generally all spectra of the series of samples agreed well with the spectrum of commercial chitosan powder (data are not shown), indicating that the chemical structure of chitosan was maintained after strong mechanical treatments.

Wide angle x-ray diffraction profiles were collected to examine the crystalline structures of the chitosan fibers after mechanical treatments. All the samples showed the same pattern and major reflection at approximately $2\theta = 11^{\circ}$ and 20°. These peaks correspond to 020 and 110 lattice planes, respectively.[36] Figure 6 shows the relative degrees of crystallinity of chitosan fibers obtained from those x-ray diffraction profiles. The degree of crystallinity gradually decreased as the number of passes increased, from 58.8% (0 pass) to 52.8% (50 passes). The decrease in crystallinity indicates that high pressure water jet treatment with 200 MPa damaged the crystalline region of chitosan nanofibers to a certain extent. The crystallinities of chitosan nanofibers with a series of passes are considerably higher than those of the 78 % DDA chitosan nanofibers (48.1% at 0 pass to 39.5% at 50 passes).[56] This is attributed to the regularity of the

polymers. Chitosan with 100 % DDA has more amine groups and could form higher number of inter and intra hydrogen bonds, which enabled the polymer to have a more regular configuration.

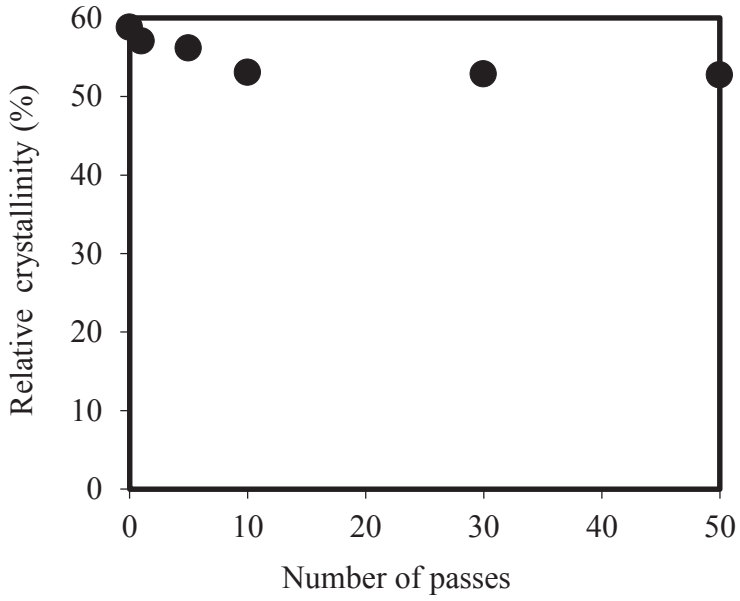

Figure 6. Degree of relative crystallinity of chitosan nanofibers as a function of the number of passes. Reproduced with permission from *International Journal of Biological Macromolecules* **2015**, *72*, 1191–1195. Copyright 2014, Elsevier.

2.3.3. Transparency and viscosity of chitosan nanofiber suspensions

The regular light transmittances with 0.1 wt. % of nanofibrillated chitosan slurries at 600 nm wavelength are shown in Figure 7. Light transmittance provides information about the morphological changes in chitosan nanofibers since fiber thickness strongly affects the transparency of the slurry. As the number of passes increased from 0 to 30 passes, the transmittance of the slurry increased steeply, from 1.7 to 50.5%. This suggests that, up to 30 passes, the chitosan fibers were disintegrated effectively. Moreover this result revealed that in between 10 and 30 passes the fibers' length decreased significantly, which facilitated the homogenous water dispersibility and light transmittance of chitosan nanofibers. However,

above 30 passes, the slope became more gradual, indicating that the nanofibers morphological change was saturated. This trend agrees with that from the SEM micrographs (Figure 5). The transparency of the slurry was slightly lower than that of the 78 % DDA chitosan nanofibers in each pass. This may be due to the difference in surface properties between these chitosan nanofibers. Since chitosan nanofibers with 100 % DDA have more regular repeating units and crystallinity, the chitosan nanofibers have lower affinity to water on the nanofiber surface, resulted in lower dispersibility and transparency in water.

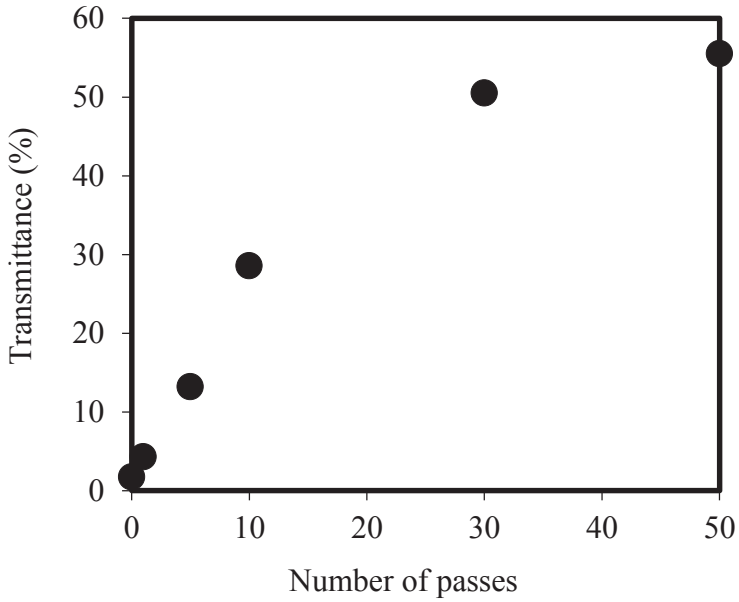

Figure 7. Regular light transmittance of chitosan nanofiber suspension at 600 nm as a function of the number of passes. Reproduced with permission from *International Journal of Biological Macromolecules* **2015**, *72*, 1191–1195.Copyright 2014, Elsevier.

Figure 8 shows the viscosities of the chitosan nanofiber slurries with 1.0 wt. % as a function of the number of passes. Viscosity was also strongly linked to the morphology of the chitosan nanofibers. The thinner and longer the nanofiber is, the higher its viscosity, because the interfibrillar interaction of nanofibers increases. The viscosity of the slurry steeply increased from 0 (178 cP) to 10 (813 cP) passes. However, above 10 passes, the viscosity linearly decreased to 440 cP at 50 passes. This trend indicates that up to10 passes, the chitosan

disintegrated well into nanofibers, which increased viscosity. Though the nanofibrillation efficiency was saturated above 10 passes, the length of nanofibers decreased by the repeated high pressure water jet treatment, which reduced viscosity.

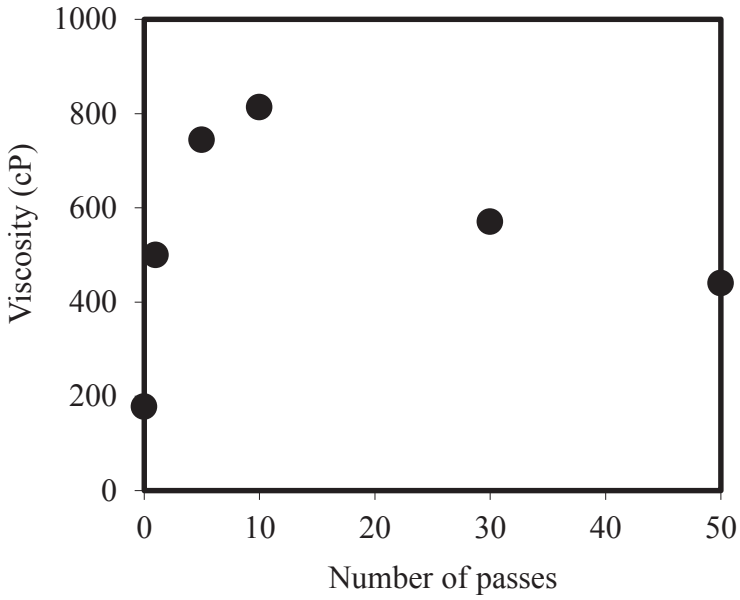

Figure 8.Viscosity of chitosan nanofiber suspension as a function of the number of passes. Reproduced with permission from *International Journal of Biological Macromolecules* **2015**, *72*, 1191–1195. Copyright 2014, Elsevier.

2.3.4. Molecular weight of chitosan nanofibers

The molecular weight of chitosan nanofibers as a function of the number of passes was estimated from the Mark- Houwink- Sakurada equation (Figure 9).[36,58] At 0 pass, chitosan possessed a molecular weight of 479 kDa. The molecular weights of the nanofibers steeply decreased from 309 kDa (1 pass) to 63 kDa (50 passes). This trend is obviously due to the depolymerization of chitosan by mechanical disintegration. The depolymerization is related to the elimination of nanofibers, as ascertained by the viscosity results (Figure 8).

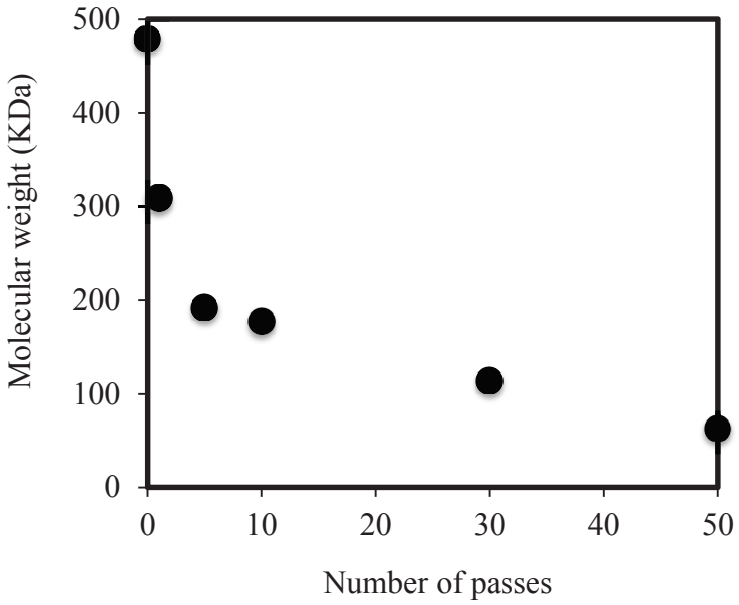

Figure 9. Molecular weight of chitosan nanofiber suspension as a function of the number of passes. Reproduced with permission from *International Journal of Biological Macromolecules* **2015**, *72*, 1191–1195. Copyright 2014, Elsevier.

2.3.5. Density and mechanical properties of chitosan nanofiber sheets

Since chitosan nanofibers could disperse homogeneously in water, nanofiber sheets were easily obtained by vacuum filtration. The thus obtained chitosan nanofiber sheets were characterized in densities and mechanical properties. The density of the chitosan nanofiber sheets gradually increased from 0.47 to 0.67 g cm^{-3} depending on the number of treatment cycles (Figure 10). Sheet density is well related to the chitosan nanofiber structure, since the thinner and shorter the chitosan nanofibers are, the more densely they can be deposited in the sheet. This trend of sheet density agreed well with that of chitosan nanofibers with 78 % DDA.

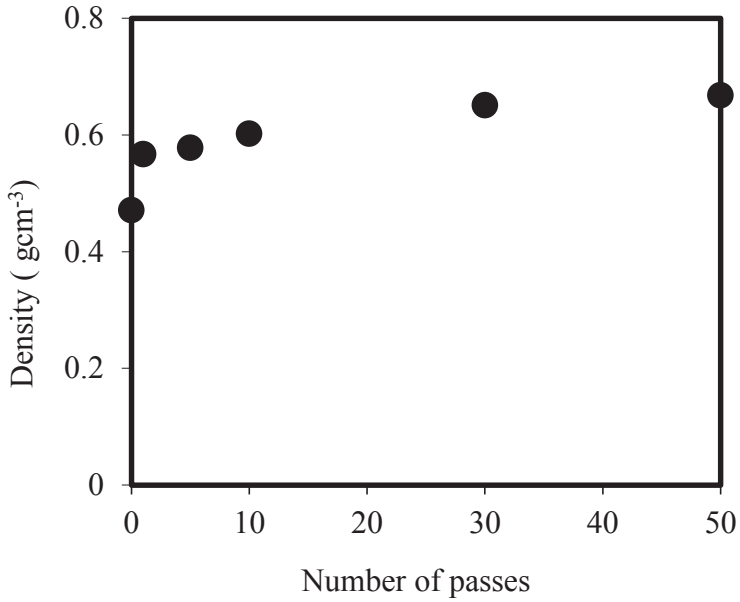

Figure 10. Density of chitosan nanofiber sheet as a function of the number of passes. Reproduced with permission from *International Journal of Biological Macromolecules* **2015,** *72*, 1191–1195.Copyright 2014, Elsevier.

Figure 11 represents the Young's moduli of chitosan nanofiber sheets graphed against the number of passes of HPWJ treatments. Young's moduli increased stably with the number of passes, from 556 MPa to1794 MPa at 0 and 50 passes, respectively. The reason for this is mainly correlated with the increase in chitosan nanofiber sheet density (Figure 10). The more densely stacked the nanofibers in the sheet could be the better to resist deformation by the applied stress. Figure 12 shows the tensile strengths of a chitosan nanofiber sheet. The tensile strengths also increased with increases in the number of passes, and reached maximum at 30 passes (30.8 MPa). However, the strength decreased by further mechanical treatment (12.2 MPa at 50 passes). As explained above excessive mechanical treatments reduced fibers' length, and obviously short nanofibers develop a structural defect and weaken the sheets' tensile strength.

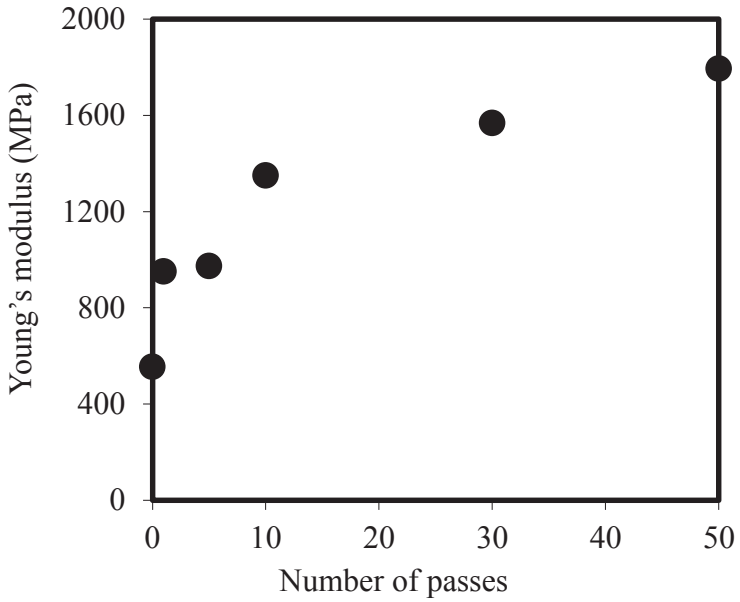

F**igure 11**. Young's modulus of chitosan nanofiber sheet as a function of the number of passes. Reproduced with permission from *International Journal of Biological Macromolecules* **2015**, *72*, 1191–1195. Copyright 2014, Elsevier.

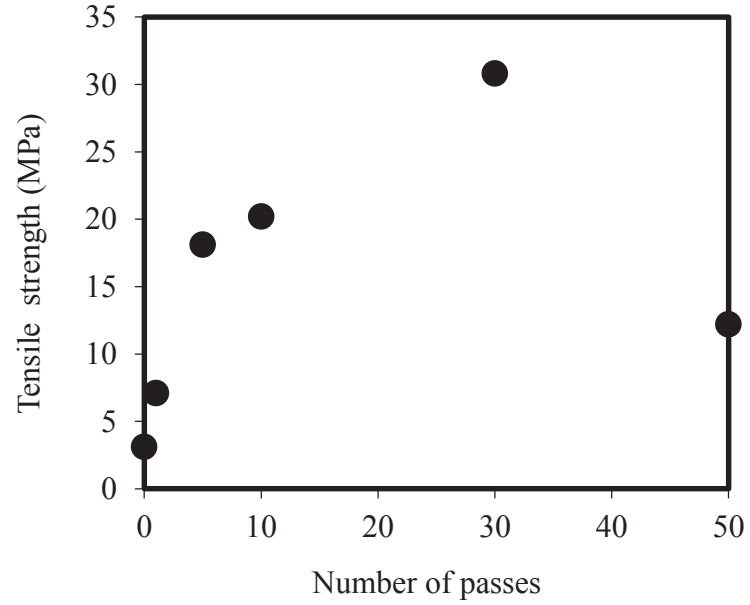

Figure 12. Tensile strength of chitosan nanofiber sheet as a function of the number of passes. Reproduced with permission from *International Journal of Biological Macromolecules* **2015**, *72*, 1191–1195. Copyright 2014, Elsevier.

2.4. Conclusion

Chitosan nanofibers were prepared from 100 % DDA dry chitosan powder using a high pressure water jet (HPWJ) system mechanical treatment. Unlike electrospinning process, in this study a top down approach was employed for the nanofibers preparation, where aggregates of fibers where converted into nanosized fibers with a high collusion force obtained by HPWJ system. The thus obtained chitosan nanofibers were characterized by their morphology, viscosity, transparency, density, chemical and crystalline structures, average molecular weight, and mechanical properties. The results were compared with those of 78 % DDA chitosan nanofibers prepared previously in the same way as the present study, but with different DDA values. Since the nanofiber aggregate structure was maintained after the deacetylation reaction, the chitosan powders were disintegrated into thinner nanofibers by mechanical treatment. As the number of passes by the HPWJ system increased, the collision force affected the chitosan nanofiber length and crystallinity. Generally the present study provided information about the possibility of making chitosan nanofibers from completely deacetylated chitosan powder using mechanical treatments, and hence it will be used to distinguish strictly between chitin and chitosan nanofibers on their biological activities.

Chapter 3

Preparation of chitin nanofibers by surface esterification of chitin with maleic anhydride and mechanical treatment

3.1. Introduction

Due to their incredible properties such as large aspect ratio, biodegradability, biocompatibility, and antibacterial activity, chitin nanofibers have been prepared using different techniques. Since commercial chitin powder consists of aggregates of nanofiber, chitin was transformed into nanofibers by mechanical processing, e.g., high pressure fluidizing,[34,35,51] disk milling,[26,32,59] ultrasonic breaking,[60-62] and powerful blender.[63,64] However, strong mechanical stress was required to disintegrate chitin into nanofibers due to the strong hydrogen bonding generated between nanofibers. Requirement of a lot of energy to obtain nanofibers by mechanical treatments raising their production cost. Thus, the development of an efficient disintegration process is indispensable to the commercial application of chitin nanofibers.

Chemical treatment can improve disintegration efficiency. Previous study reported that chitin nanocrystals were easily prepared by TEMPO mediated oxidation of α-chitin.[28] Carboxylate groups were formed by the oxidation of chitin at the C-6 primary hydroxyl group on the nanofiber surface, facilitating mechanical disintegration with the assistance of the osmotic pressure effect. More recently it was also described that lignocellulose nanofibers were prepared by the esterification of wood flour with maleic anhydride.[65] Carboxylate groups were generated by the esterification of hydroxyl groups at the C2, 3, and 6 positions of cellulose. The introduced carboxylate groups facilitated nanofibrillation and significantly reduced the

energy required to produce lignocellulose nanofibers. Inspired by these previous works, the author here studied the facile mechanical disintegration of commercially available chitin powder into nanofibers by chemical treatment with maleic anhydride. Since chitin also has hydroxyl groups at the C3 and C6 positions, it would be esterified also by maleic anhydride, and generating a carboxylate group on chitin enables the facile conversion of chitin into nanofibers by the subsequent mechanical treatment.

3.2. Experimental

3.2.1. Materials

Chitin powder from crab shell with a 6.4 % degree of deacetylation (DDA) was purchased from Koyo Chemical Industry (Hyogo, Japan) and used without further purification. Maleic anhydride was purchased from Nacalai Tesque (Kyoto, Japan) and used as received.

3.2.2. Esterification of α-chitin with maleic anhydride

Chitin was esterified with maleic anhydride by referring the previous method.[65] The scheme for preparing the esterified chitin nanofiber is shown in Figure 13. Dry chitin powder (6 g) from crab shell reacted with maleic anhydride (30 g) at 120 ^{o}C for 3.5 h with occasional stirring. The reactant was collected by filtration and washed with acetone and then with pure water thoroughly until the filtrate became neutral. To neutralize the introduced maleate groups, approximately 10–15 mL of 1.0 M NaOH aqueous solution was added to the esterified chitin water dispersion until the pH of the solution reached 11. The excess NaOH was then removed by washing with pure water until the pH of the suspension became 7.8. The final concentration of the esterified chitin dispersion was 1.29 wt. %. The sample was stored in the refrigerator.

The experimental yield was estimated by gravimetric analysis.

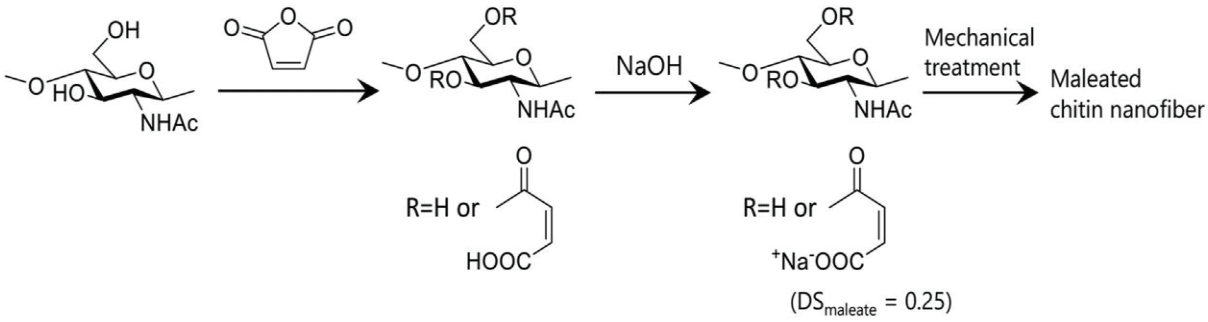

Figure 13. Preparation scheme for the surface maleated chitin nanofiber. Reproduced with permission from *Carbohydrate Polymers* **2016**, *153*, 55–59. Copyright 2016, Elsevier.

3.2.3. Mechanical disintegration of maleated chitin dispersion

The esterified chitin was diluted with water at 0.5 wt. %, and the dilute dispersion was treated with a grinder (MKCA6-3; Masuko SangyoCo., Ltd., Kawaguchi, Japan) twice. The grinder treatment was performed at 1500 rpm with a clearance gauge of -1.5 (corresponding to a 0.15 mm shift) from the zero position, which was determined as the point of slightest contact between the grinding stones. In principle, there is no direct contact between the stones due to the presence of chitin suspension. For comparison purpose unmodified chitin in acidified water was mechanically crushed with the same cycles of grinder treatment as esterified chitin nanofibers. The thus obtained nanofibers were characterized and the results were compared.

3.2.4. Maleated chitin nanofibers film preparation

Esterified chitin nanofiber dispersion was diluted with deionized water at 0.1 wt. % concentration. After removal of dissolved gases under vacuum, the aqueous dispersion was casted on Teflon plates and dried in the oven at 50°C until the dried films detached from the plates by themselves. Similar steps were used for the preparation of unmodified chitin

nanofibers film.

3.2.5. Characterization

3.2.5.1. Morphological observation of esterified and unmodified chitin nanofibers

The morphology of maleated and unmodified chitin nanofibers was determined using field emission scanning electron microscopic (FE-SEM). The nanofiber dispersions were diluted with an excessive amount of ethanol and dried in an oven. The dried samples were coated with an approximately 2 nm layer of platinum using an ion sputter coater and were observed by FE-SEM (JSM-6700F; JEOL, Ltd) operating at 2.0 kV.

3.2.5.2. Determination of chemical and crystalline structure of maleated and unmodified chitin nanofibers

For chemical structure elucidation the infrared spectra of the samples were recorded with an FT-IR spectrophotometer (Spectrum 65, Perkin-Elmer Japan, and Tokyo, Japan) equipped with an ATR attachment. The x-ray diffraction profiles were obtained using x-ray goniometer scanning from 5^{o} to 60^{o} with Ni-filtered CuKα from an x-ray generator (Ultima IV; Rigaku, Tokyo, Japan) operating at 40 kV and 40 mA. The crystallinity indices (CI) of the samples were calculated from the ratio of the area of four crystalline peaks derived from (020), (110), (120), and (130) plane to the total area between 2 $\theta = 5^{o}$ to 30^{o}.[66] The esterified chitin nanofibers' crystal sizes at (020) and (110) reflection planes were measured from the widths at half heights of the diffraction peaks, using Scherrer's equation.[67]

3.2.5.3. Light transmittance and zeta potential measurements of maleated and unmodified chitin nanofibers

The light transmittances of 0.1wt. % nanofiber dispersions and the self-standing films were measured using a UV–vis spectrophotometer (V550; JASCO, Tokyo, Japan). The zeta potential of aqueous esterified and unmodified chitin nanofiber dispersions at 0.5 wt. % was measured using a laser-Doppler method apparatus (ELSZ-1000ZS, Otsuka Electronics, and Hirakata, Japan). Five measurements were considered to calculate the average zeta potential value of each sample.

The degree of substitution (DS) of the maleate group introduced on the nanofiber surface was calculated from the C and N weight percentages obtained from an elemental analyzer (Vario, EL III; Elementar, Hanau, Germany) according to: C/12.01:N/14.01= (8 + 4n):1, where C and N are the weight percentages of carbon and nitrogen atoms obtained from the elemental analysis and n is the molar ratio of the DS values of the introduced maleate groups against the N-acetyl glucosamine unit of the nanofiber. Electrical conductivity titration method was also applied to determine DS.[28]

3.3. Results and discussion

3.3.1. Preparation of esterified chitin nanofibers

Dry α-chitin powder was reacted with neat maleic anhydride at 120 ºC for 3.5 h (Figure 13). Although maleic anhydride is solid at room temperature, it melts above 52.6 ºC, enabling a solventless reaction, which offers the advantages of low cost, ease of purification, a high reaction rate, and environmental friendliness. It is known that acid anhydride is preferentially

introduced into high reactive amino group.[59] Thus, maleyl group was at first introduced into amino group, slightly existing on chitin nanofiber in prior to hydroxyl group with lower reactivity. And then, maleic anhydride could form ester linkages with primary hydroxyl group at C6 position preferentially due to steric hindrance, thus forming a carboxylic acid group (-COOH). After the reaction, the introduced carboxylic acid was neutralized by NaOH to change it into carboxylate salt ($-COO^{-}Na^{+}$). The esterified chitin and unmodified chitin were treated with the grinder twice to disintegrate them into nanofibers. After the mechanical treatment, the esterified chitin was homogeneously dispersed in water, and the dispersion was highly transparent compared to the unmodified chitin (Figure 14). The regular light transmittances of esterified and unmodified chitin dispersions in water with a 0.5 wt. % concentration at 600 nm were 91.5 % and 13.1 %, respectively. To elucidate the dispersion property of esterified chitin nanofiber in water, the dispersion was centrifuged at 10,000 rpm for 10 min. After the precipitate was removed, the yield of nanofibers in the supernatant fraction was 97.2 % in weight. The high dispersion ability comes from the surface property of the esterified chitin. The average zeta potential of the esterified chitin dispersion at pH 7.8 was -48.41 ± 9.6 mV. The high negative surface charge is obviously attributable to the carboxylate anion (COO^{-}). The strong negative charge enabled homogeneous dispersion. Original chitin nanofiber with $+54.7 \pm 15.4$ mV zeta potential at pH 3.0 can disperse homogeneously in acidic water. Slight amino groups on the chitin enable stable dispersion of nanofiber by electrostatic repulsion. On the other hand, the chitin nanofiber precipitate in basic water immediately. Thus, esterified chitin with stable dispersion in basic water allows for the chemical reaction under basic condition or compounding with basic materials.

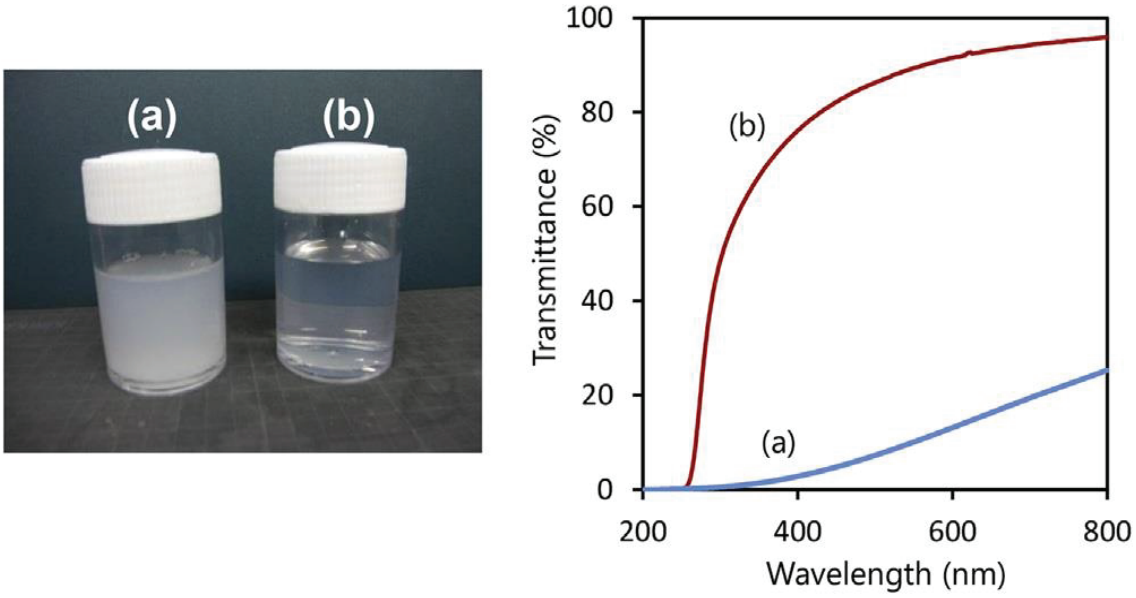

Figure 14. Photograph and UV–vis spectra of (a) untreated and (b) maleated chitin nanofiber dispersions. Reproduced with permission from *Carbohydrate Polymers* **2016**, *153*, 55–59. Copyright 2016, Elsevier.

Figure 15a and b are SEM images of nanofibers obtained from esterified chitin with different magnification. After two cycles of simple disk milling treatment, the esterified chitin was easily and completely disintegrated into homogeneous nanofibers over an extensive area. As determined from the SEM images of 50 randomly selected nanofibers, the average thickness of maleated chitin ananofibers was about 10 nm. The disintegration efficiency of the esterified chitin was much higher than that of the unmodified chitin (Figure 15c). Nanofibers in the unmodified chitin were thicker and heterogeneous. The thicknesses varied widely from 10 to 100 nm. The average diameter was about 45 nm. The great difference in morphology indicates that the carboxylate group of the esterified chitin helped the mechanical disintegration. Anionic charges on the fiber surface brought about interfibrillar electrostatic repulsion and osmotic pressure, facilitating mechanical disintegration.

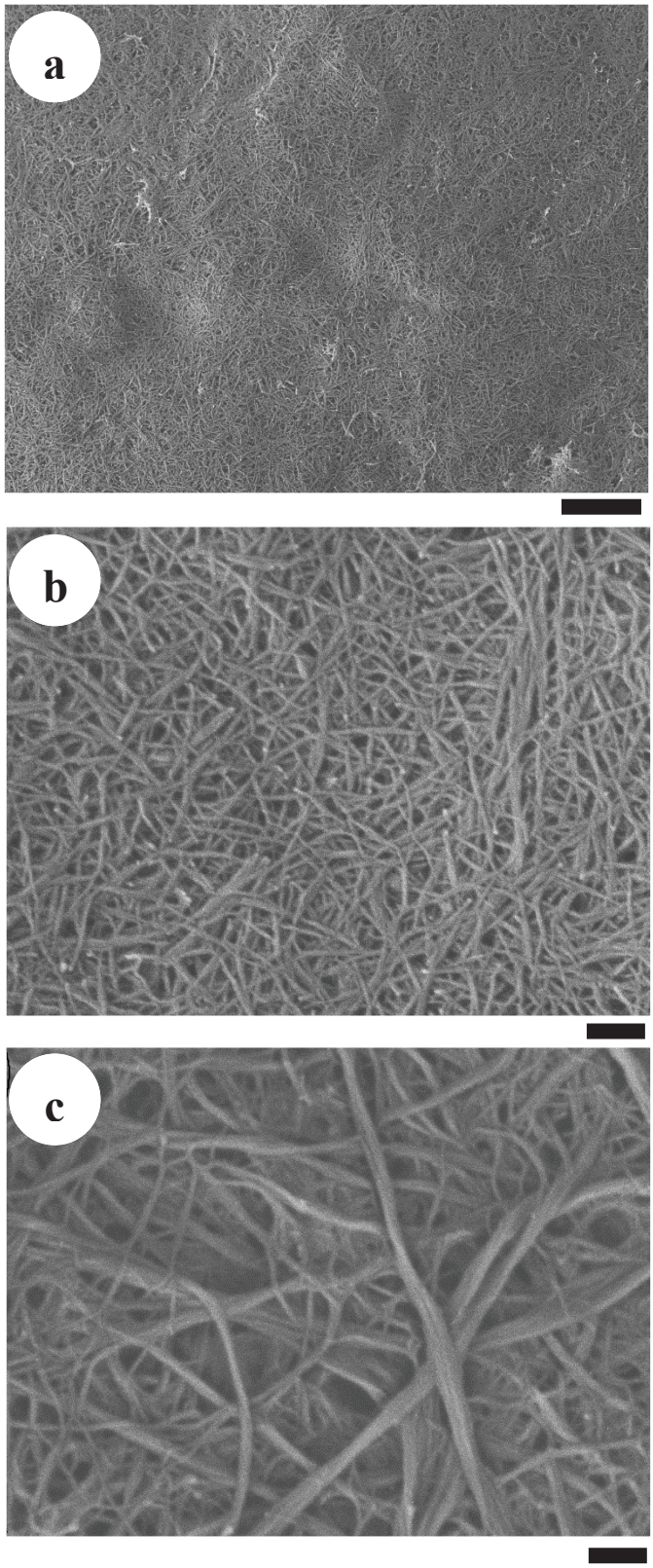

Figure 15. SEM images of (a and b) esterified and (c) unmodified chitin nanofiber. Scale bar: (a) 1000 nm, (b and c) 200 nm. Reproduced with permission from *Carbohydrate Polymers* **2016**, *153*, 55–59. Copyright 2016, Elsevier.

3.3.2. Characterization of esterified chitin nanofibers

The degree of substitution (DS) of the maleate group of the esterified chitin nanofibers, as determined by the elemental analysis of C and N atoms, was 0.25, which means that one fourth of the N-acetyl glucosamine unit was reacted with maleic anhydride. The reaction was highly reproducible at the same reaction conditions. However, from the first trial experiment the author noticed that the DS value of the maleate group was strongly affected by the reaction time and temperature. For example, when chitin was esterified at 100 ^{o}C for 2 h, the DS was 0.15. The difference in DS value affected transparency of the maleated nanofibers, in which lower DS maleated chitin nanofibers dispersion or film possessed lower transmittance values.

After the esterification, the weight of the chitin increased to 6.17 g from 6.00 g. Since the theoretical weight of the esterified chitin with 0.25 DS was 6.64 g, the percentage yield of the esterified chitin was 93 % in weight. This indicates that the reaction is suitable for producing chitin nanofibers without significant mass loss during the process. Electrical conductivity titration method was also applied to determine the DS. The DS was 0.21, which was slightly lower than that from elemental analysis. The difference indicates that nanofibers were completely esterified on the surface. Moreover, inner amorphous part of nanofiber was also partially esterified.

FT-IR spectra of the esterified chitin nanofibers thus prepared were shown in Figure 16. The amide I bands at 1652 cm^{-1} and 1620 cm^{-1}, and the amide II band at 1556 cm^{-1} are characteristic peaks of α-chitin. This suggests the esterification reaction and subsequent mechanical treatment did not affect the chemical structure of original chitin nanofibers. In addition, the peak at 1722 cm^{-1} is derived from the C=O stretching vibration mode of the maleate moiety. This newly appeared absorption band is an evidence for the introduction of the

maleate groups into the chitin nanofibers. The absence of absorption peaks at around 1787 and 1857 cm^{-1}, which related to the ring anhydride carbonyl group showed that no maleic anhydride remained in the sample.

X-ray diffraction patterns of maleylated chitin nanofibers are shown in Figure 17. The diffraction peaks at approximately 9.4°, 19.5°, 20.7°, and 23.1° were in good agreement with those of the typical antiparallel crystalline pattern of α-chitin, which corresponds to (020), (110), (120), and (130) planes, respectively.[37] The relative crystallinity of esterified chitin nanofibers estimated from the comparison between crystalline and total diffraction areas was 74 %, which is slightly higher than unmodified chitin (68 %). The slight increase in the relative crystallinity of maleated chitin nanofibers may be attributed to the reduction of peak areas contributed by the amorphous diffractions. Maleic anhydride preferentially reacted with amorphous region and esterified amorphous was removed by washing process. Moreover, maleate groups were introduced onto the surface and the amorphous part of the nanofibers, and that the original chitin crystalline structure was maintained after the esterification reaction. The mean crystal sizes of the esterified nanofibers estimated by XRD patterns were 6.8 nm and 5.4 nm at (020) and (110) planes, respectively.

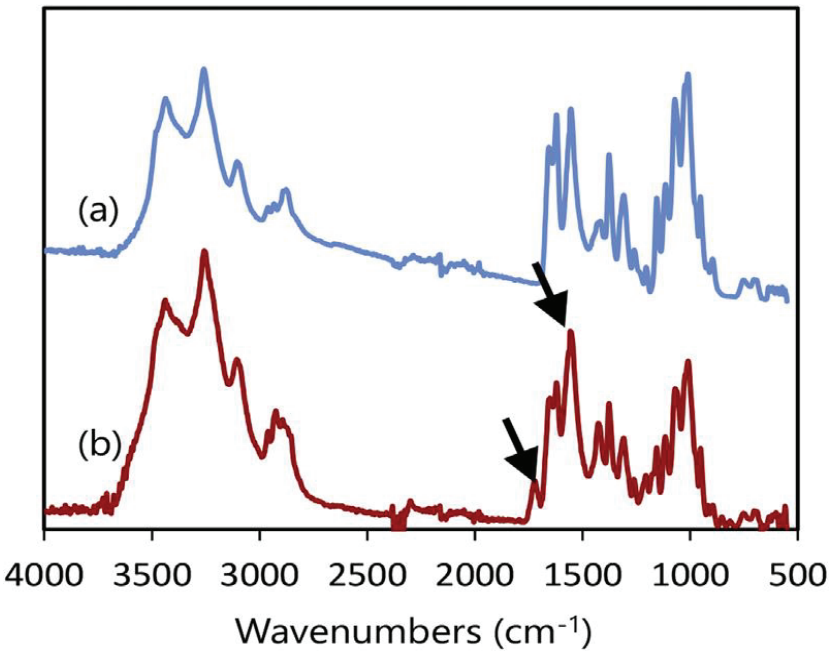

Figure 16. FT-IR spectra of (a) unmodified and (b) maleated chitin nanofibers. Reproduced with permission from *Carbohydrate Polymers* **2016**, *153*, 55–59. Copyright 2016, Elsevier.

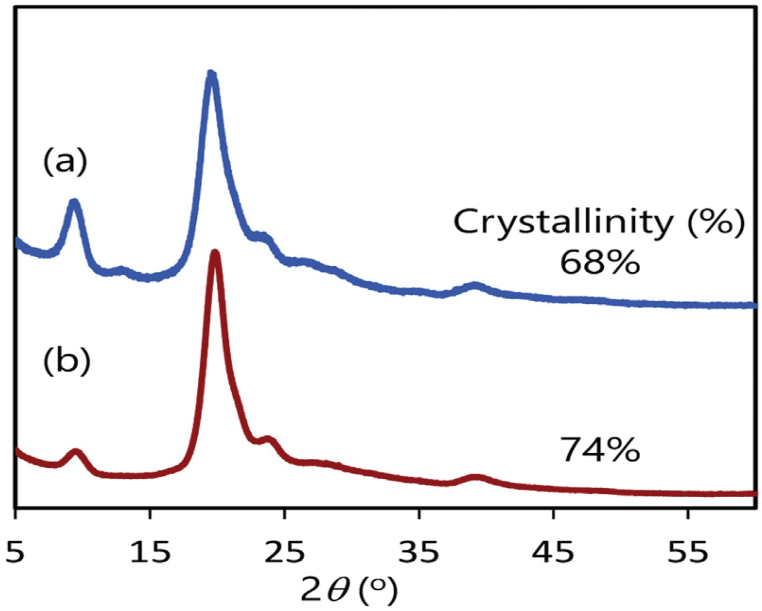

Figure 17. X-ray diffraction profiles of (a) unmodified and (b) maleated chitin nanofibers. Reproduced with permission from *Carbohydrate Polymers* **2016**, *153*, 55–59. Copyright 2016, Elsevier.

The author prepared a cast film using the maleated and unmodified chitin nanofiber dispersions. The cast film resulted from the maleated chitin nanofibers dispersion had a much higher transparency than that from the unmodified chitin nanofiber (Figure 18). The regular light transmittances of the esterified and unmodified chitin nanofiber films at 600 nm were 74.4 % and 2.4 %, respectively. The significant difference in transparency is due to the differences in their nanofiber thickness and water dispersibility. That is, the esterified nanofibers that were narrower and more dispersible in water could be slowly concentrated by the evaporation of the water so that nanofibers were piled up uniformly and gradually. The nanofibers, which were so densely stacked that cavities in the cast film were almost completely removed. Since the cast film was free from light scattering in the sheet, it became more transparent.[68]

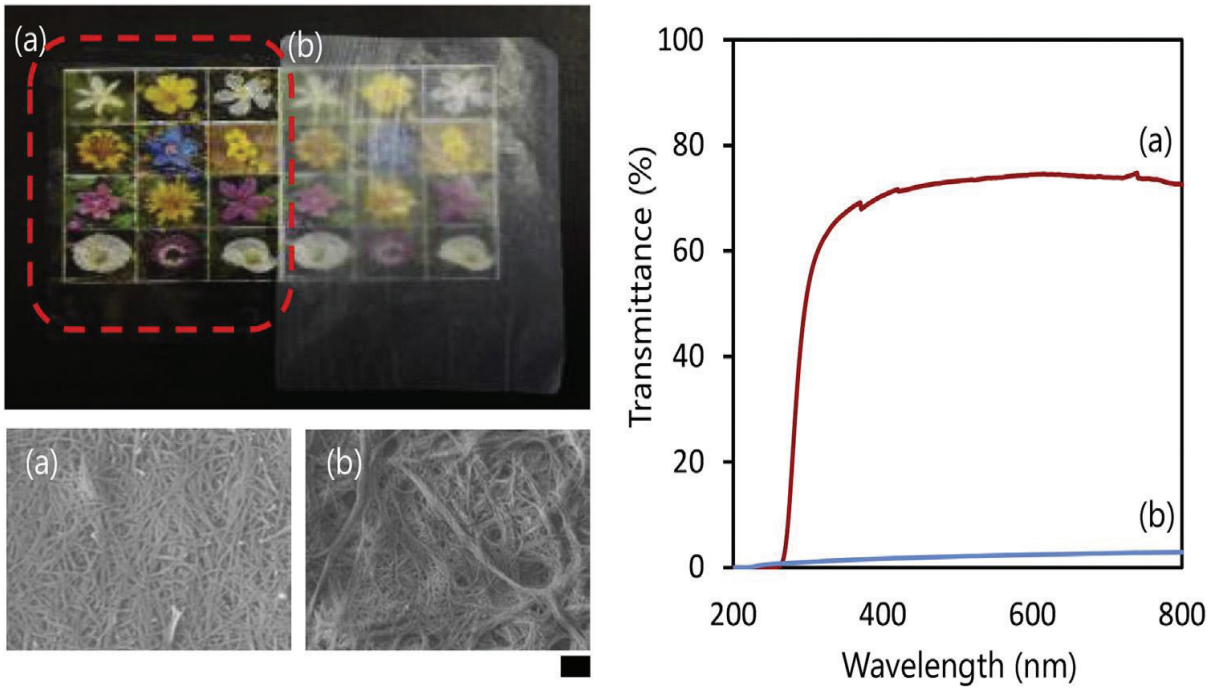

Figure 18. Appearances, SEM images, and UV–vis spectra of (a) maleated and (b) unmodified chitin nanofiber film. Scale bar: 200 nm. Reproduced with permission from *Carbohydrate Polymers* **2016**, *153*, 55–59. Copyright 2016, Elsevier.

3.4. Conclusion

Esterified chitin nanofibers with 0.25 DS were successfully prepared by the reaction of chitin with neat maleic anhydride and subsequent mechanical disintegration without losing its crystalline structure. The introduced maleate groups significantly facilitated the mechanical disintegration due to the strong electrostatic repulsion and osmotic pressure. The surface carboxylate group enhanced the nanofibers' homogeneous dispersion property in water at higher pH, which enabled me to obtain a highly transparent film by a casting method. The author expected that chitin nanofibers with an anionic hydrophilic functional group, a uniform nanofiber morphology, and a very high surface ratio will be available as a novel nanobiomaterial that can function in a variety of applications.

Chapter 4

Protein/$CaCO_3$/chitin nanofiber complex prepared from crab shells by simple mechanical treatment and its effect on plant growth

4.1. Introduction

Chitin is a highly abundant carbohydrate polymer occurring primarily in crab and shrimp shells. The rigid chitin molecules are aligned in an antiparallel manner to form α-chitin nanofibers with an extended crystalline structure. These nanofibers are covered by a protein layer. The next layer consists of clusters of protein/chitin nanofibers that form a twisted plywood layer, which is gradually rotated about its normal axis. Calcium carbonate, consisting of calcite crystal, is embedded in the small cavity of the helicoidally shaped structure. Chitin nanofibers have a characteristic morphology,[31] high surface to volume ratio,[69] high mechanical strength,[70,71] and efficient biological properties.[72-75]

The chitin in crab shells is partially preserved in the fishing industry as an intermediate of chitosan and glucosamine, even though the other parts of the shell are disposed of as industrial waste. Chitin can be prepared from crab shells by treatment with NaOH and HCl aqueous solutions to remove proteins and calcium carbonate, respectively.[1] A major effluent purification process is then required to purify the abundant calcium carbonate and protein residue, and the expense of this process is passed on in the cost of commercial chitin (currently about 5000 Japanese Yen/kg). In a previous study, a method was developed for skipping the protein removal process to bring down production costs.[76] The protein/chitin nanofiber

complex thus obtained could reinforce acrylic resin film and increased its mechanical properties. Moreover, the protein layer on the chitin nanofiber behaved as a substrate for the biomineralization of calcium carbonate. On the basis of that study, it was hypothesized that there might be a possibility to convert the chitin in crab shells into nanofiber directly, without removing the protein and calcium carbonate. Simplification of the preparation process would significantly reduce the production cost of nanofiber. Furthermore, eliminating the use of chemicals for purification would make the process more environmentally friendly. In this study, the author reported on the direct disintegration of crab shells into nanofibers using previously proposed method.[76] Then the obtained protein/$CaCO_3$/chitin nanofiber complex was characterized in detail, and its potential application as a plant fertilizer was discussed since it is well known that crab shells show enhancement of plant growth.

4.2. Experimental

4.2.1. Materials

The raw shells of Chionoecetes opilio (red snow crab) and α-chitin powder with a 6.4 % deacetylation degree were obtained from Koyo Chemicals. Other chemicals were purchased from Aldrich or Kanto Chemicals and were used as received. Tomato seeds were purchased from the Marutane Seed Co.,Ltd., Kyoto, Japan.

4.2.2. Preparation of the protein/$CaCO_3$/chitin nanofiber complex

Raw crab shells were roughly crushed with a domestic blender under wet conditions. The crushed sample was then disintegrated with a grinder (MKCA6-3; Masuko Sanyo Co., Ltd., Kawaguchi, Japan) at 1500 rpm for two cycles. The air bubbles were removed by a super stirrer

(Awatori-rentaro, ARE-301, THINKY, Ltd., Tokyo, Japan). The concentration of the total solid was adjusted to 3.6 wt. % for a chitin weight percentage of around 1 wt. %. The samples were then passed through a high pressure water jet (HPWJ; Star Burst Mini, HJP-25001S, Sugino Machine, Namerikawa, Japan) system equipped with a ball collision chamber. The slurry was ejected from a small nozzle with a diameter of 100 μm under high pressure of 200 MPa. This mechanical treatment was repeated for 1, 5, 10, 30, and 50 cycles.

4.2.3. Preparations of the protein/chitin nanofiber complex and pure chitin nanofiber

Protein/chitin nanofiber complex and pure chitin nanofiber were prepared and their effects on tomato growth were compared with that of the protein/$CaCO_3$/chitin nanofiber complex. The protein/chitin nanofiber complex was prepared using the previously reported procedure with slight modifications.[76] Briefly, the raw crab shells were crushed with a domestic blender under wet condition. The crushed sample was treated with 2 M hydrochloric acid for two days at room temperature, with occasional stirring to remove mineral salts (mainly calcium carbonate). The sample was collected by filtration and washed with deionized water until the filtrate became neutral. Then it was disintegrated by 2 cycles grinder treatment, and the concentration of the overall solid was adjusted to 1.15 wt. %. The ground sample was passed through 5 and 50 cycles of a high-pressure water jet (HPWJ) system. For comparison, pure chitin nanofibers were also prepared as described in the previous study with little modification.[34] In brief, dry pure chitin powder was dispersed in water at 1 wt. %. After 1 h of stirring, the dispersion was crushed with a grinder for two cycles. The crushed sample was stirred under a vacuum for 1 h to remove air bubbles. Finally, it was mechanically homogenized with 5 and 50 cycles of the HPWJ system. Furthermore, a crab shell was roughly crushed with a domestic blender and dispersed in water at chitin concentration of 1 wt. % and its effect for tomato plant growth was compared with the mineralized chitin-protein nanofiber complex.

4.2.4. Characterization

4.2.4.1. Morphological characterization of protein/$CaCO_3$/chitin complex nanofiber

For morphological observation, the disintegrated samples were diluted with ethanol and dried in an oven. The dried samples were coated with an approximately 2 nm layers of platinum, using an ion sputter coater, and were observed by an FE-SEM (JSM-6700F; JEOL, Ltd) operating at 2.0 kV. The same procedure was employed for the morphological characterization of protein/chitin nanofibers after removing $CaCO_3$ component from the complex.

4.2.4.2. Structural determination of protein/$CaCO_3$/chitin complex nanofiber

To determine the chemical structure of the complex nanofibers, the infrared spectra of the samples were recorded with an FT-IR spectrophotometer (Spectrum 65; Perkin-Elmer Japan, Yokohama, Japan) equipped with an ATR attachment (diamond/ZnSe crystal) with four scans at a spectral resolution of 4 cm^{-1}.

4.2.4.3. Light transmittance and viscosity measurements of protein/$CaCO_3$/chitin complex nanofiber

The light transmittances of the protein/$CaCO_3$/chitin nanofiber complex dispersion were measured using a UV-Vis spectrophotometer (V550; JASCO, Tokyo, Japan). The viscosities of the complex slurries were determined with a Brookfield digital viscometer DV-E using the LV-4 spindle (Brookfield Engineering Laboratories, Middleboro, MA, USA) at 30 ^oC.

The protein, calcium carbonate, and chitin contents of the original crab shells were estimated by means of a ninhydrin-hydrindantin protein test[77] and gravimetric analysis.

Calcium carbonate and protein were separated from the crab shells by conventional 1 M HCl and 1 M KOH treatments, respectively.

4.2.4.4. Plant material

Tomato (Solanum lycopersicum) cv. Chibikko (Marutane Seed) was grown hydroponically with rockwool grow cubes (AO 36/40; Grodan). Three weeks after seedling, the tomato plants were treated once per week with a series of nanofibers, which contained chitin at a final concentration of 0.01 % to each rockwool cube. The number of true leaves, the stem diameter (at cotyledon node), and the plant height (stems length above the cotyledon) were measured after the fifth and ninth nanofiber treatments. Soil plant analysis development (SPAD) reading using chlorophyll meter SPAD-502 plus (Konica Minolta, Japan) was taken twice around the midpoint near the midrib of second young leaf sample and averaged. The plants were grown under environmentally controlled conditions with 14 h of light/10 h of dark cycles at 25 ^{o}C, and treated with nanofibers once a week. Distilled water (DW) was used as a negative control, and commercial nutrition HYPONeX (N-P-K = 6-10-5; Hyponex Japan, Osaka, Japan) at a concentration of 0.001 % was used as a positive control.

4.3. Results and discussion

4.3.1. Preparation and characterization of the protein/$CaCO_3$/chitin nanofiber Complex

Red snow crab shells were used as a starting material in this study. The contents of the main components in the crab shells (chitin, protein, and calcium carbonate) were estimated by the ninhydrin-hydrindantin protein test and gravimetric analysis, and they were approximately 30 %, 16 %, and 55 % as w/w, respectively, indicating the largest proportion of the red crab

shells was calcium carbonate. Figure 19 shows field emission scanning electron microscope (FE-SEM) images of a crab shell after high pressure water jet (HPWJ) treatments with 0, 1, 5, 10, 30, and 50 passes. Before HPWJ treatment (Figure 19a), the crab shell organization consisted of protein/chitin nanofiber bundles with calcium carbonate. After one pass treatment (Figure 19b), the organization had partially disintegrated, and nanosized fibers were observed to some extent. The morphological changes in the crab shell after one pass treatment were due to strong mechanical load of the HPWJ treatment. When the number of passes increased from 5 to 50, the fiber's width decreased further due to fibrillation of the protein/chitin nanofiber bundle. Calcium carbonate grains also disintegrated into smaller nanoparticles. Thus, the protein/$CaCO_3$/chitin nanofiber complex was successfully obtained from crab shells by HPWJ mechanical treatments.

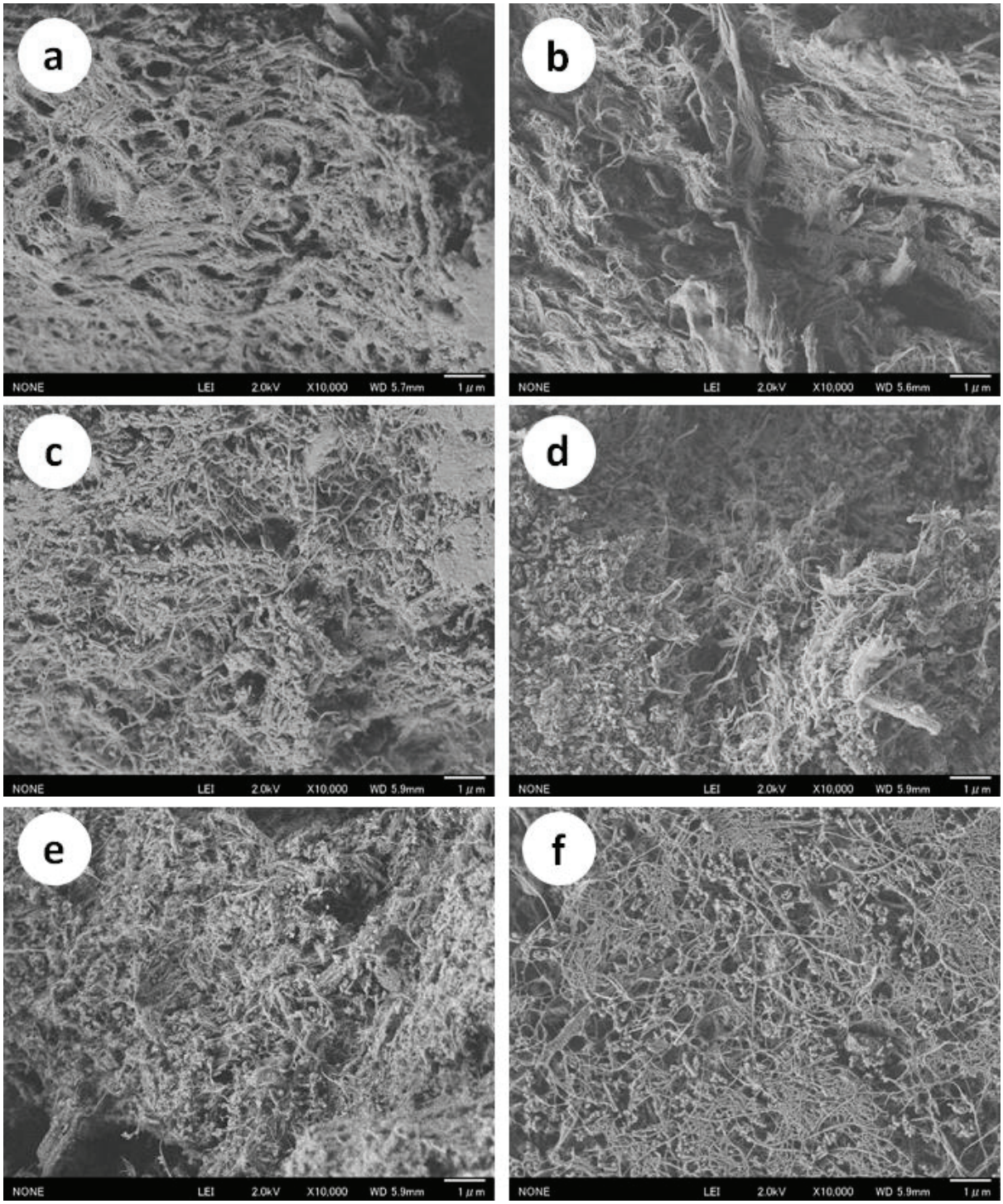

Figure 19. FE-SEM micrographs of crab shells after (a) 0, (b) 1, (c) 5, (d) 10, (e) 30, and (f) 50 passes through the high pressure water jet system. The scale bar length is 1 μm. Reproduced with permission from *International Journal of Molecular Sciences* **2016**, *17*, 1600. Copyright 2016, MDPI.

To further characterize the morphology of the nanofiber, calcium carbonate was removed from samples treated with 0, 1, and 5 passes of HPWJ system. Each sample was neutralized by HCl and calcium carbonate was dissolved in water as $CaCl_2$. SEM images revealed that nanofibrillation of the crab shells proceeded by repeated HPWJ treatments and appeared complete at 5 passes (Figure 20c).

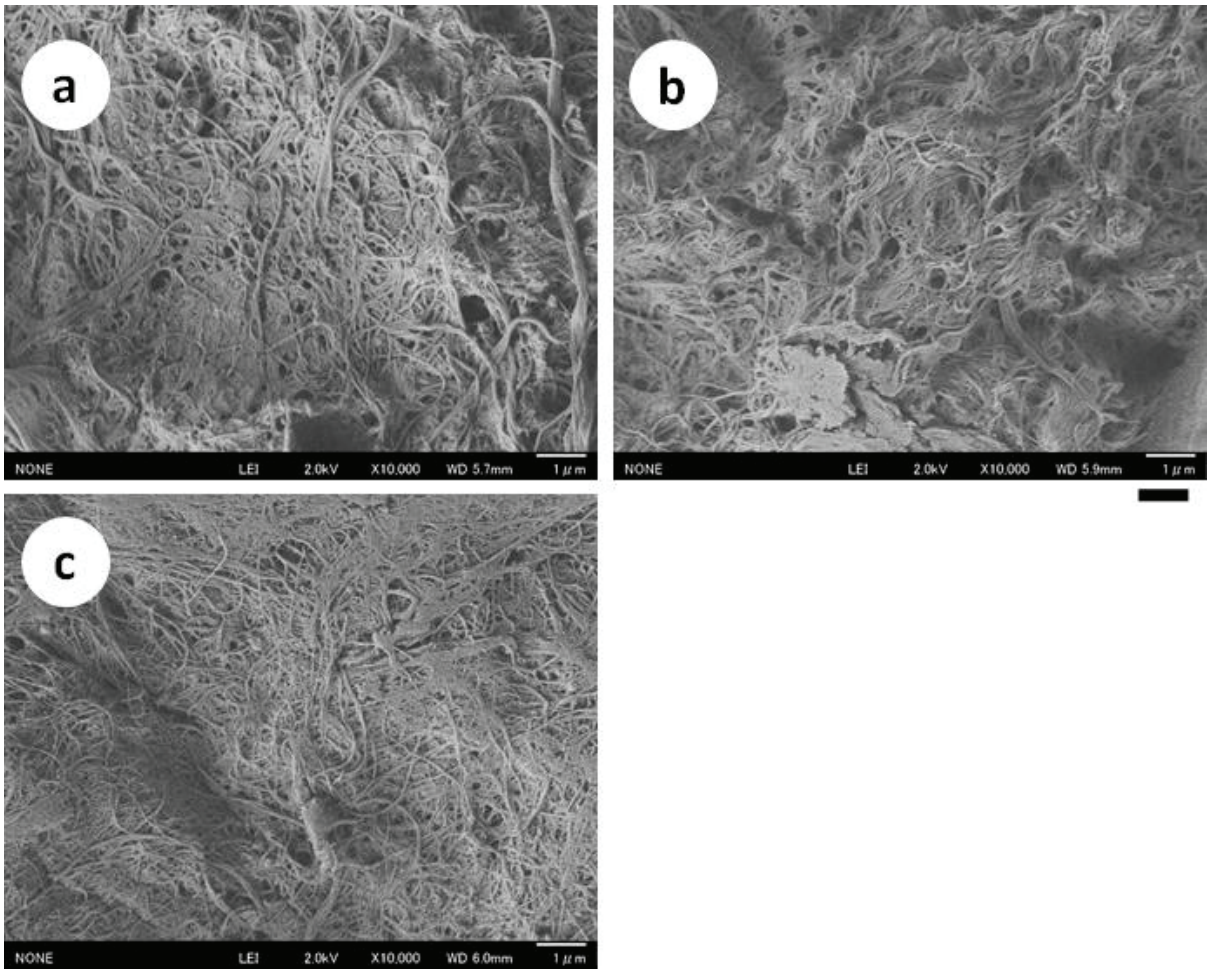

Figure 20. FE-SEM micrographs of crab shells with (a) 0, (b) 1, and (c) 5 cycle treatments through the high pressure water jet system after removal of $CaCO_3$. The scale bar length is 1 μm. Reproduced with permission from *International Journal of Molecular Sciences* **2016**, *17*, 1600. Copyright 2016, MDPI.

Figure 21 shows the FTIR-ATR spectra of pure chitin, calcium carbonate, and crab shells treated by the HPWJ system after 0, 1, 5, 10, 30, and 50 passes. All spectra of the mechanically treated crab shells were in excellent agreement with each other. This suggests that the original chemical structures of the crab shells were maintained after HPWJ mechanical treatments. In particular, the OH stretching band at 3424 cm^{-1}, NH stretching band at 3259 cm^{-1}, amide I bands at 1652 and 1621 cm^{-1}, and amide II band at 1554 cm^{-1} of the chitin nanofibers were observed. These bands are the characteristic absorption peaks of α-chitin.[1] Bands at approximately 870 and 1450 cm^{-1} were derived from the vibrations of calcium carbonate.[78] On the other hand, the peaks corresponding to protein were not observed, due to the weak nature of the protein bands compared to their chitin and $CaCO_3$ counterparts.

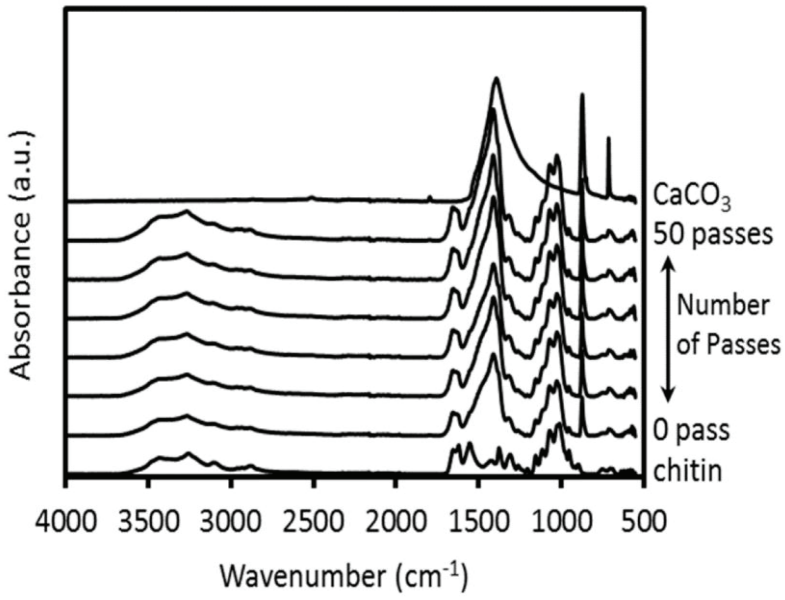

Figure 21. FTIR-ATR spectra of pure chitin, calcium carbonate, and crab shells treated with 0, 1, 5 10, 30, and 50 passes through a high pressure water jet system. Reproduced with permission from *International Journal of Molecular Sciences* **2016**, *17*, 1600. Copyright 2016, MDPI.

Figure 22 shows the light transmittances of a 0.1 wt. % concentration, mechanically treated crab shell of water dispersion at 800 nm. The transmittance values were highly

reproducible. Transparency is strongly associated with chitin fiber thickness because, when the solid fibers are dispersed at the nano level, the suspension becomes transparent.[79] After HPWJ treatment, the crab shells remained well-dispersed in water for at least one month. Thus, the crab shells were easy to handle and shape into the desired forms. Without HPWJ treatment, the light transmittance of crab shells was only 9.6 %. As the number of passes increased, the thickness of the nanofibers decreased; and consequently, the light transmittance of the dispersion increased. At 1 and 5 passes, the transmittance increased steeply to 12.7 % and 17.1 %, respectively. This shows that the composite nanofibers revealed high morphological change up to 5 passes. Above 10 passes, the transparency did not change significantly, reaching only 25.5 % at 50 passes. This trend indicates that up to five times mechanical treated fibers were fibrillated into thinner nanofibers, thus increasing their transparency. However, above 5 passes, the nanofibers were mostly fully fibrillated and further disintegration was difficult resulting in saturated transparency. These trends well agreed with the morphology of the complex nanofiber obtained by FE-SEM (Figure 19).

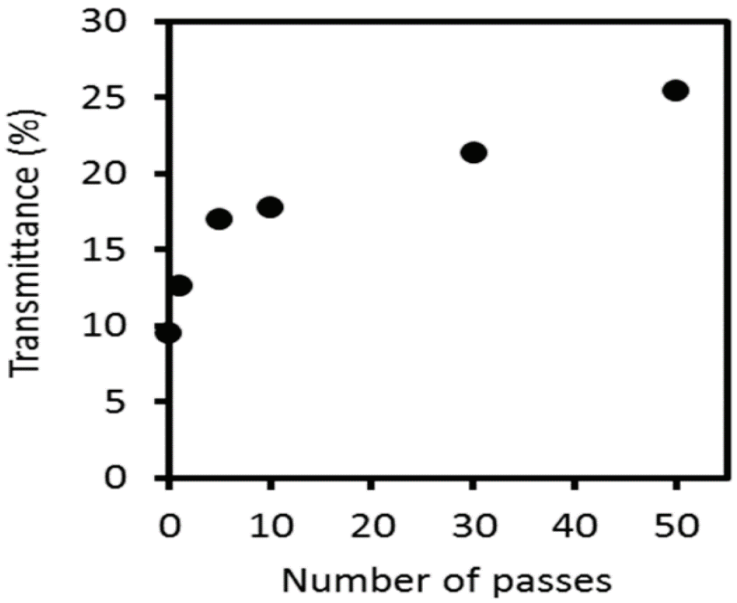

Figure 22. Regular light transmittances of protein/$CaCO_3$/chitin nanofiber dispersions at 800 nm as a function of the number of passes. Reproduced with permission from *International Journal of Molecular Sciences* **2016**, *17*, 1600. Copyright 2016, MDPI.

Figure 23 shows the viscosities of 3.6 wt. % mechanically treated crab shell dispersions as a function of the number of passes. The repeated measurements were highly reproducible. The viscosity of the slurry sharply increased from 3380 centipoise (cP) at zero pass to 9633 cP at 5 passes. However, above 5 passes the viscosity decreased constantly to 2860 cP at 50 passes. Viscosity is strongly affected by nanofiber's morphology.[35] Up to 5 passes of HPWJ treatment the nanofibers became thinner and longer, resulted in increasing the slurries' viscosity. On the other hand approximately over 5 passes the nanofibrillation was mostly ended and instead the fiber's length decreased as fibers started to break by the high pressure collision force; thereby lowering the viscosity. Based on the SEM observations, transparency, and viscosity measurement results, it could be inferred that the crab shell composite fibers were properly disintegrated and nanofibrillated at around 5 passes of HPWJ treatment.

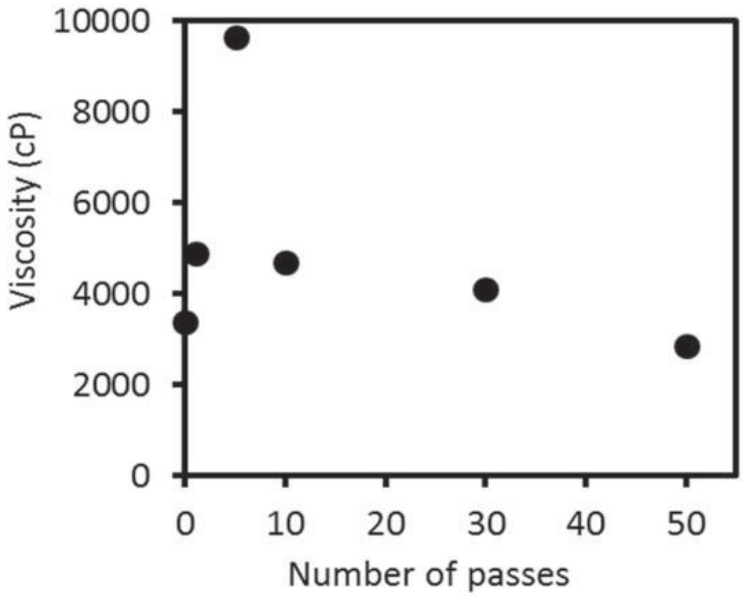

Figure 23. Viscosity of protein/$CaCO_3$/chitin nanofiber dispersions as a function of the number of passes. Reproduced with permission from *International Journal of Molecular Sciences* **2016**, *17*, 1600. Copyright 2016, MDPI.

4.3.2. Effect of protein/$CaCO_3$/chitin nanofiber complex on tomato growth

Tomato plants grown in a hydroponic system were treated with nanofibers once a week. After the fifth nanofiber treatment, the tomato plants treated with protein/$CaCO_3$/chitin nanofibers exhibited markedly higher number of leaves, stem diameter, and plant height than the controls (Figure 24, Table 2). The effect of the crab shell powder on the tomato plant growth was comparable to that of mineralized chitin-protein composite nanofibers. As noted in Table 2, after the fifth and ninth treatments, the effects of crab shell powder were not significantly different at ($p < 0.05$) from those of protein/$CaCO_3$/chitin nanofibers with respect to the number of leaves and stem diameter of the plants. However, the effects of the two supplements on the height of the tomatoes after five times treatments were significantly different at ($p < 0.05$); where the protein/$CaCO_3$/chitin nanofibers exhibiting the better effect on tomato growth. The difference was attributed to the fast release of minerals deposited in the nanofibers network to the hydroponics system as a result of mechanical treatment. Moreover, after 9 times nanofibers treatment their soil plant analysis development (SPAD) values were also significantly different. SPAD readings are used to assess leaf chlorophyll concentration, and estimate nitrogen content. The positive correlation between SPAD value and nitrogen content in tomato leaves has been reported.[80] SPAD values of tomato leaves treated with mineralized chitin-protein composite nanofibers were higher than those treated by roughly crushed crab shell (Table 2). The result indicated that nitrogen content must be higher in the tomato leaves treated by mineralized chitin-protein composite nanofibers, since mechanical treatment significantly facilitated the release of nitrogen to the hydroponic system for plant uptake. From this it can be concluded that the high nitrogen status in the tomato plants treated by mineralized chitin-protein composite nanofibers should positively affect plant growth in the late stages. In addition, mechanically disintegrated protein/$CaCO_3$/chitin nanofibers were easy to apply due to their liquid state, compared to the insoluble, roughly crushed crab shell powder.

On the other hand, neither protein/chitin nanofibers nor chitin nanofibers had any effect on tomato growth. Tomato plants treated with protein/chitin nanofiber, chitin nanofiber and distilled water (DW) died at the ninth nanofibers treatment; whereas tomato plants treated with protein/$CaCO_3$/chitin nanofibers or crab shells showed healthy growth. These results indicated that the protein/$CaCO_3$/chitin nanofibers might act as a fertilizer. Plants require not only essential elements such as nitrogen, phosphorus, and potassium but also calcium, sulfur, magnesium, and trace minerals for their growth. Although chitin nanofibers and protein/chitin nanofibers contain essential nitrogen, these nanofibers might not contain sufficient amounts of minerals to promote plant growth. Even though the effects of protein/$CaCO_3$/chitin nanofibers were not as dramatic as those of the commercial nutrient HYPONeX; after further improvements in treatment, the complex nanofibers might show good performance as a fertilizer. The results in Table 2 also revealed that there were no significant differences among the nanofibers treated with a different number of passes of the HPWJ system in terms of tomato growth. Therefore, the 0 pass sample of protein/$CaCO_3$/chitin nanofibers, which was roughly disintegrated by grinder treatment with two passes, might be a cost effective material for use as a fertilizer for plant growth.

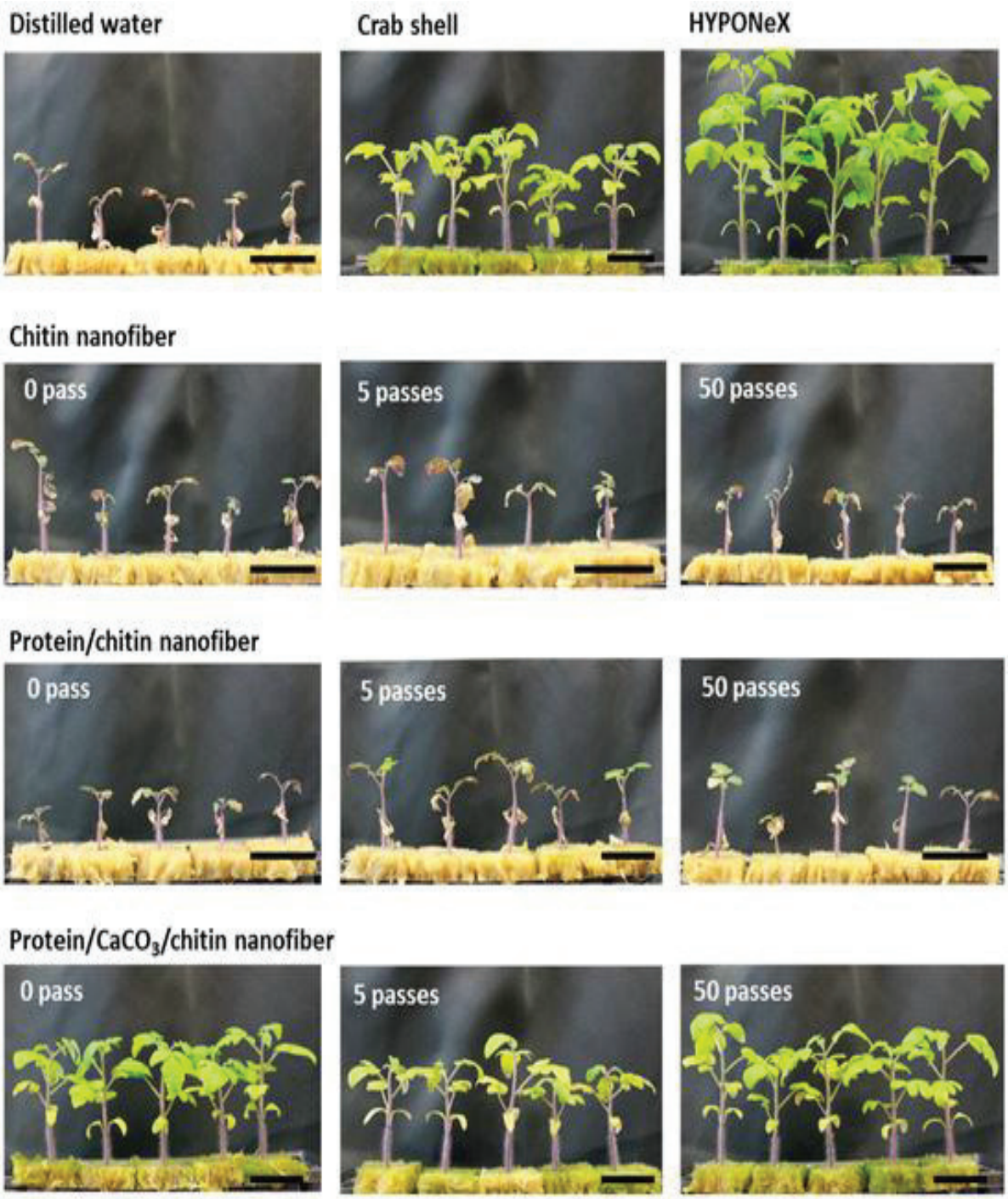

Figure 24. Tomato plants grown hydroponically with nanofibers treatment. Tomato plants were treated with chitin nanofiber, protein/chitin nanofiber, and protein/$CaCO_3$/chitin nanofiber at a final concentration of chitin 0.01 %. The series of nanofibers were prepared with high pressure water jet treatment with 0, 5, and 50 passes. The photo was taken after the fifth nanofiber treatment. Distilled water was administered as a negative control and commercial nutrition (HYPONeX) as a positive control. Roughly-crushed crab shell powder was treated as a control. The scale bar length is 36 mm. Reproduced with permission from *International Journal of Molecular Sciences* **2016**, *17*, 1600. Copyright 2016, MDPI.

Table 2. The effect of protein/$CaCO_3$/chitin nanofibers on the growth of tomato plants.

Day after treatment	Treatment	Number of mechanical treatment (passes)	Number of leaves	Stem diameter (mm)	Plant height (cm)	SPAD value
5 weeks	Distilled water	-	3.2±0.1 ^{a}	1.4±0.0 ^{a}	0.9±0.1 ^{a}	NT
	HYPONeX	-	8.3±0.2 ^{b}	3.0±0.2 ^{b}	11.6±0.8 ^{b}	NT
	Crab shell	-	6.0±0.3 ^{c}	2.0±0.1 ^{c}	4.3±0.2 ^{c,d,e}	NT
	Protein/CaCO3/ chitin nanofiber	0	6.3±0.2 ^{c}	2.2±0.1 ^{c}	6.8±1.9 ^{c}	NT
		5	5.8±0.3 ^{c}	2.0±0.1 ^{c}	4.4±0.4 ^{c,d}	NT
		50	6.7±0.2 ^{c}	2.2±0.1 ^{c}	5.0±0.1 ^{c}	NT
	Protein/chitin nanofiber	0	3.1±0.2 ^{a}	1.4±0.0 ^{a}	1.0±0.1 ^{a}	NT
		5	3.5±0.2 ^{a}	1.5±0.0 ^{a}	1.4±0.1 ^{a,d,e}	NT
		50	3.6±0.2 ^{a}	1.5±0.0 ^{a}	1.2±0.1 ^{a,e}	NT
	Chitin nanofiber	0	3.2±0.1 ^{a}	1.4±0.0 ^{a}	1.0±0.1 ^{a}	NT
		5	3.0±0.3 ^{a}	1.4±0.0 ^{a}	1.0±0.1 ^{a}	NT
		50	3.0±0.1 ^{a}	1.4±0.0 ^{a}	0.9±0.0 ^{a}	NT
9 weeks	Distilled water	-	ND	ND	ND	ND
	HYPONeX	-	9.7±0.4 ^{a}	3.3±0.1 ^{a}	16.6±0.5 ^{a}	36.0
	Crab shell	-	8.4±0.5 ^{a}	2.1±0.1 ^{b}	7.0±0.9 ^{b}	33.1
	Protein/CaCO3/ chitin nanofiber	0	9.1±0.3 ^{a}	2.2±0.1 ^{b}	9.1±0.6 ^{b}	37.7
		5	8.6±0.3 ^{a}	2.2±0.1 ^{b}	7.8±0.6 ^{b}	36.5
		50	9.2±0.3 ^{a}	2.3±0.1 ^{b}	9.3±0.5 ^{b}	36.7
	Protein/chitin nanofiber	0		ND		
		5		ND		
		50		ND		
	Chitin nanofiber	0		ND		
		5		ND		
		50		ND		

Data represent the mean of four independent experiments and standard error. Means with the same letter are not significantly different according to Tukey's test ($P < 0.05$) in each week. ND (not detectable) indicates dead plant. NT (Not tested).

4.4. Conclusion

A protein/$CaCO_3$/chitin nanofiber complex was prepared from crab shells using a simple mechanical treatment. Since the complex nanofiber preparation process did not include the conventional protein and calcium carbonate removal processes, it could bring down the production cost and environmental load. The obtained protein/$CaCO_3$/chitin nanofiber complex would be available as a fertilizer to improve plant growth in hydroponic systems. Indeed, the mineral part of the nanofiber complex was found to be vital for plant growth and maturation. Finally, the novel nanofiber complex could be prepared at a low cost through an eco-friendly process. Thus, the results of this close analysis of the unique nanofiber complex characteristics could lead to more effective utilization of crab shell waste.

General summary

Biomaterials have gained attractiveness in the last decades due both environmental and economic concerns. The intensive use of petroleum based resources results in not only their significant depletion but also brings a negative contribution to climate changes on the planet. Cellulose and chitin are the most abundant, biodegradable and renewable polysaccharides extracted from plant and animal sources, respectively. Due to the rapidly growing field of bio-nanotechnology, biobased nanofibers are getting tremendous attention by the scientific community. Two different approaches have been used for nanofibers preparation from these natural polysaccharides. The first one is the bottom- up approach, in which monomeric units come together and form a large polymer. The most common technique of this approach is electrospinning process. However, bionanofibers obtained by the second approach (top-down) have superior qualities in terms of crystallinity, reproducibility, biodegradability and biocompatibility. Recently mechanical treatments are becoming the common methods as a top-down approach for the isolation of bionanofibers from their polysaccharide sources.

The present study is focused on the preparations of nanofibers from chitin and its derivatives using mechanical treatments. The resulted nanofibers were characterized in details. Moreover, the obtained nanofibers applications as plan fertilizer was investigated. The study had given much attention for the environmental and economic issues.

In chapter 1, the author reported the effect of grinder pretreatments for easy disintegration of chitin into nanofiber by subsequent HPWJ treatments. The SEM micrographs, viscosity data and transmittance measurements revealed that pre-grinder treatments remarkably reduced the subsequent number of passes by HPWJ system for complete nanofibrillation of α-

chitin. The aggregated chitin passed through both the G-1 and G-2 pre-grinder treatments underwent complete nanofibrillation at around 5 passes of HPWJ treatments. On the other hand non pre-grinder treated samples showed complete nanofibrillation at around 10 passes of HPWJ treatments. The result clearly indicates that pre-grinder treatments are essential to reduce the energy and time needed for complete nanofibrillation of chitin by the subsequent HPWJ treatments. This demonstrated that the production cost of chitin nanofibers using HPWJ system can be decreased nearly by half. Therefore, the present finding may increase the production of chitin nanofibers in large scale using mechanical treatments with reasonable price.

Chapter 2 demonstrated the preparation of chitosan nanofibers from 100 % deacetylated chitosan powder using mechanical treatments. Since the properties of chitosan is strongly affected by its degree of deacetylation (DDA), in this study nanofibers from completely deacetylated chitosan were prepared and characterized in terms of their morphology, transparency, viscosity, mechanical strength and chemical and crystalline structures. As the SEM micrographs revealed chitosan fibrillation improved with increasing number of passes by HPWJ system, and nanofibrillation was completed at around 10 passes. Relative crystallinity of chitosan nanofibers gradually decreased as the number of passes increased since HPWJ treatment damaged the crystalline region of chitosan nanofibers. The molecular weights of the nanofibers steeply decreased due to the depolymerization of chitosan by mechanical disintegration. The density of chitosan nanofiber sheets were increased with increasing number of treatments by HPWJ system. Sheet density is well related to the chitosan nanofibers structure, since the thinner and shorter the chitosan nanofibers are, the more densely they can be deposited in the sheet. The Young's modulus and tensile strength of chitosan nanofibers sheets were enhanced as the number of treatments by the HPWJ increased, but further treatments deteriorated the tensile strength.

In chapter 3, the author described the facile preparation of chitin nanofibers by surface esterification of chitin with maleic anhydride and mechanical treatment. A simple and solventless reaction procedure was employed to introduce the maleate groups on the surface of chitin, which will have both economic and environmental benefits for large scale production of chitin nanofibers. Usually 2 passes pre-grinder and minimum of 5 passes subsequent HPWJ treatments are needed for the complete nanofibrillation of α-chitin in acidic solution. However, in this study a uniform nanofibers with an average thickness of 10 nm were obtained by applying only 2 passes grinder treatment in a basic water. The nanofibrillation was facilitated by the electrostatic repulsions between the introduced carboxylate groups. Unlike the unmodified chitin nanofibers, the maleated chitin nanofibers were homogenously dispersed in water at neutral or basic pH, which will be useful to use the product in non-acidic environments. Both the esterification reaction and subsequent grinder treatments did not affect the chemical and crystalline structures of original chitin.

Chapter 4 denoted the preparation of protein/$CaCO_3$/chitin nanofiber complex from crab shells by simple mechanical treatment and its effect on tomato growth. The complex nanofiber was obtained without the application of hazardous chemicals to remove the mineral and protein components. Hence, the preparation procedure was both cost effective and environmentally friendly. The crab shell was first roughly crushed by 2 passes grinder treatment and disintegrated into nanofibers using the strong mechanical load of HPWJ system. As the transparency and viscosity data revealed maximum morphological change was observed at around 5 passes of HPWJ system. From the SEM micrographs of mineralized nanofiber complex, it is almost impossible to see at which passes nanofibrillation was completed due to the embedded calcium carbonate nanoparticles. On the other hand, the SEM images of chitin/protein complex nanofibers just after removing $CaCO_3$ component revealed that a thin and excellent nanofibers networking were observed at 5 passes of HPWJ treatment.

The mineralized protein/ chitin nanofiber complex was used as a fertilizer for the growth of tomato in the hydroponic system. Tomato plants treated with mineralized chitin-protein composites displayed substantial increased in the number of leaves, stem diameter and height. The roughly crushed crab shell powder has shown also the same effect, however; mechanically disintegrated mineralized chitin/protein nanofiber complex depicted a better effect on the height and nitrogen content of tomatoes. Moreover, mechanically disintegrated mineralized nanofiber complex can be controllably applied to the hydroponic system since it has a liquid state, compared to the insoluble roughly crushed crab shell powder. The result clearly indicated that with further adjustment in its treatment, the mineralized chitin-protein composite nanofibers might have a great potential to replace chemical fertilisers, which are costly and environmentally unfriendly.

References

(1) Nair, K.G.; Dufresne, A. Crab shell chitin whisker reinforced natural rubber nanocomposites.1. Processing and swelling behavior. *Biomacromolecules* **2003**, *4*, 657–665.

(2) Einbu, A.; Naess, S.N.; Elgsaeter, A.; Vårum, K.M. Solution properties of chitin in alkali. *Biomacromolecules* **2004**, *5*, 2048–2054.

(3) Gooday, G. W. The ecology of chitin degradation. *Advances in Microbial Ecology* **1990**, *11*, 387–430.

(4) Garner, K.H.; Blackwell, J. Refinement of the structure of beta chitin. *Biopolymers* **1975**, *14*, 1581–1595.

(5) Rinaudo, M. Chitin and chitosan: properties and applications. *Progress in Polymer Science* **2006**, *31*, 603–632.

(6) Paillet, M.; Dufresne, A. Chitin whisker reinforced thermoplastic nanocomposites. *Macromolecules* **2001**, *34*, 6527–6530.

(7) Morin, A.; Dufresne, A. Nanocomposites of chitin whiskers from Riftia tubes and Poly (caprolactone). *Macromolecules* **2002**, *35*, 2190–2199.

(8) Rao, M.S.; Munoz, J.; Stevens, W.F. Critical factors in chitin production by fermentation of shrimp biowaste. *Applied Microbiology and Biotechnology* **2000**, *54*, 808–813.

(9) Kurita, K. Chitin and chitosan: functional biopolymers from marine crustaceans. *Marine Biotechnology* **2006**, *8*, 203–226.

(10) Morganti, P.; Morganti, G. Chitin nanofibers for advanced cosmeceuticals. *Clinics in Dermatology* **2008**, *26*, 334–340.

(11) Muzzarelli,R.A.;Boudrant,J.;Meyer,D.; Manno, N.; DeMarchis,M.;Paoletti, M.G. Current views on fungal chitin/chitosan, human chitinases, food reservation, glucans, pectins and inulin attribute to Henri Braconnot, precursor of the carbohydrate polymer sscience, on the chitin bicentennial. *Carbohydrate Polymers* **2012**, *87*,995–1012.

(12) Younes, I.; Ghorbel-Bellaaj, O.; Chaabouni M. et al., Use of a fractional factorial design to study the effects of experimental factors on the chitin deacetylation. *International Journal of Biological Macromolecules* **2014**, *70*, 385–390.

(13) Liu X.F.; Guan,Y. L.; Yang, D. Z.; Li, Z.; Yao, K.D. Antibacterial action of chitosan and carboxymethylated chitosan. *Journal of Applied Polymer Science* **2001**, *79*, 1324–1335.

(14) Freier, T.; Koh, H.S.; Kazazian, K.; Shoichet, M.S. Controlling cell adhesion and degradation of chitosan films by N-acetylation. *Biomaterials* **2005**, *26*, 5872–5872.

(15) Cao, W.L.; Jing, D.H.; Li, J.M.; Gong, Y.D.; Zhao, N.M.; Zhang, X.F. Effects of the degree of deacetylation on the physicochemical properties and Schwann cell affinity of chitosan films. *Journal of Biomaterials Applications* **2005**, *20*,157–177.

(16) Hidaka, Y.; Ito, M.; Mori, K.; Yagasaki, H.; Kafrawy, A.H. Histopathological and immunohistochemical studies of membranes of deacetylated chitin derivatives implanted over rat calvaria. *Journal of Biomedical Materials Research Part A,* **1999**, *46*, 418–423.

(17) Kittur, F. S.; Vishu Kumar, A. B.; Tharanathan, R. N. Low molecular weight chitosans Preparation by depolymerization with Aspergillus niger pectinase and characterization. *Carbohydrate Research* **2003**, *338*, 1283–1290.

(18) Ramakrishna, S.; Fujihara, K.; Teo, W.E.;Yong, T.; Ma, Z.; Ramaseshan, R. (2006). Electrospun nanofibers: Solving global issues. *Materials Today* **2006**, *9*, 40–50.

(19) Feng, C.; Khulbe, K.C.; Matsuura, T. Recent progress in the preparation, characterization, and applications of nanofibers and nanofiber membranes via electrospinning/interfacial polymerization. *Journal of Applied Polymer Science* **2010**, *115*, 756–776.

(20) Huang, Z.M.; Zhang, Y.Z.; Kotaki, M.;Ramakrishna, S. A review on polymer nanofibers by electrospinning and their applications in nano composites. *Composites Science and Technology* **2003**, *63*, 2223–2253.

(21) Subbiah, T.; Bhat, G.S.; Tock, R.W.; Parameswaran, S.; Ramkumar, S.S. Electrospinning of nanofibers. *Journal of Applied Polymer Science* **2005**, *96*, 557–569.

(22) Dai, Y.; Liu, W.; Formo, E.; Sun, Y.; Xia, Y. Ceramic nanofibers fabricated by electrospinning and their applications in catalysis, environmental science, and energy technology. *Polymers for Advanced Technologies* **2011**, *22*, 326–338.

(23) Ifuku, S.; Saimoto , H. Chitin nanofibers: preparations, modifications, and applications. *Nanoscale* **2012**, *4*, 3308–3318.

(24) Raabe, D.; Romano P.; Sachs, C.; Fabritius, H.; Al-Sawalmih, A.; Yi, S.-B.; Servos, G.; Hartwig, H.G. Microstructure and crystallographic texture of the chitin-protein network in the biological composite material of the exoskeleton of lobster Homarus americanus. *Materials Science and Engineering: A* **2006**, *421*, 143–153.

(25) Chen, P.-Y.; Lin, A. Y.-M.; McKittrick, J.; Meyers, M. A. Structure and mechanical properties of crab exoskeletons. *Acta Biomaterialia* **2008**, *4*, 587–596.

(26) Ifuku, S.; Nogi, M.; Abe, K.; Yoshioka, M.; Morimoto, M.; Saimoto, H.; Yano, H. Preparation of Chitin nanofibers with a uniform width as α-chitin from crab shells. *Biomacromolecules* **2009**, *10*, 1584–1588.

(27) Revol, J.F.; Marchessault, R. H. In vitro chiral nematic ordering of chitin crystallites. *International Journal of Biological Macromolecules* **1993**, *15*, 329–335.

(28) Fan, Y.; Saito, T.; Isogai, A .Chitin Nanocrystals Prepared by TEMPO-Mediated Oxidation of α-Chitin. *Biomacromolecules* **2008**, *9*, 192–198.

(29) Zhao, H. P.; Feng, X. Q.; Gao, H. Ultrasonic technique for extracting nanofibers from nature materials. *Applied Physics Letters* **2007**, *90*, 073112.

(30) Min, B. M.; Lee, S. W.; Lim, J. N.; You, Y.; Lee, T. S.; Kang, P. H.; Park, W. H. Chitin and chitosan nanofibers: electrospinning of chitin and deacetylation of chitin nanofibers. *Polymer* **2004**, *45*, 7137–7142.

(31) Ifuku, S.; Nogi, M.; Yoshioka, M.; Morimoto, M.; Yano, H.; Saimoto, H. Fibrillation of dried chitin into 10-20nm nanofibers by a simple grinding method under acidic conditions. *Carbohydrate Polymers* **2010**, *81*, 134–139.

(32) Ifuku, S.; Nogi, M.; Abe, K.; Yoshioka, M.; Morimoto, M.; Yano, H.; Saimoto, H. Simple preparation method of chitin nanofibers with a uniform width of 10-20 nm from prawn shell under neutral conditions. *Carbohydrate Polymers* **2011**, *84*, 762–764.

(33) Ifuku, S.; Nomura, R.; Morimoto, M.; Saimoto, H. Preparation of chitin nanofibers from mushrooms. *Materials* **2011**, *4*, 1417–1425.

(34) Ifuku, S.; Yamada, K.; Morimoto, M.; Saimoto, H. Nanofibrillation of dry chitin powder by star burst system. *Journal of Nanomaterials* **2012**, *2012*, 1–7.

(35) Dutta, A.K.; Yamada, K.; Izawa, H.; Morimoto, M.; Saimoto, H.; Ifuku, S. Preparation of chitin nanofibers from dry chitin powder by star burst system: Dependence of number of passes. *Journal of Chitin and Chitosan Science* **2013**, *1*, 59–64.

(36) Zhang,Y.; Xue, C.; Xue, Y.; Gao, R.; Zhang, X. Determination of the degree of deacetylation of chitin and chitosan by x-ray powder diffraction. *Carbohydrate Research* **2005**, *340*, 1914–1917.

(37) Minke, R.; Blackwell, J. The structure of α-chitin. *Journal of Molecular Biology* **1978**, *120*, 167–181.

(38) Peter, M.G. Applications and environmental aspects of chitin and chitosan. *Journal of Macromolecular Science Part A* **1995**, *32*, 629–640.

(39) Rao, S.B.; Sharma, C.P. Use of chitosan as a biomaterial: studies on its safety and hemostatic potential. *Journal of Biomedical Materials Research* **1997**, *34*, 21–28.

(40) Muzzarelli, R.A.A. Chitin formation and diagenesis. *Gupta, S.N., (Ed.), Springer, Dordrecht, the Netherlands*, **2011**, *34*, 1–34.

(41) Muzzarelli, R.A.A.; Boudrant, J.; Meyer, D.; Manno, N.; DeMarchis, M.; Paoletti, M.G. Current views on fungal chitin/chitosan, human chitinases, food preservation, glucans, pectins and inulin: A tribute to Henri Braconnot, precursor of the carbohydrate polymers science, on the chitin bicentennial. *Carbohydrate Polymers* **2012**, *87*, 995–1012.

(42) Muzzarelli, R.A.A. Nanochitins and nanochitosans paving the way to eco-friendly and energy saving exploitation of marine resources in*: K. Maty-jaszewski, M. Möller (Eds.), Polymer Science: A Comprehensive Reference, Elsevier, Amsterdam*, **2012**, *10*, 153–164.

(43) Huang, Z.M.; Zhang, Y.Z.; Kotaki, M.; Ramakrishna. S. A review on polymer nanofibers by electrospinning and their applications in nanocomposites. *Composites Science and Technology* **2003**, *63*, 2223–2253.

(44) Sill, T.J.; Recum, H.A. Electrospinning: applications in drug delivery and tissue engineering. *Biomaterials* **2008**, *29*, 1989–2006.

(45) Lee, K.Y.; Jeong, L.; Kang, Y.O; Lee, S. J;Park, W. H. (2009). Electrospinning of polysaccharides for regenerative medicine. *Advanced Drug Delivery Reviews* **2009**, *61*, 1020-1032.

(46) Min, B.; Lee, S.W.; Lim, J.N.; You, Y.; Lee, T.S.; Kang, P.H.; Park, W.H. Chitin and chitosan nanofibers: electrospinning of chitin and deacetylation of chitin nanofiber. *Polymer* **2004**, *45*, 7137–7142.

(47) Supaphol, P.; Suwantong, O.; Sansanoh, P.; Sowmya, S.; Jayakumar, R.; Nair, S.V. Electrospinning of biocompatible polymers and their potentials in biomedical applications. *Advances in Polymer Science* **2012**, *246*, 213–240.

(48) Jayakumar, R.; Prabaharan, M.; Nair, S.V.; Tamura, H. Novel chitin and chitosan nanofibers in biomedical applications. Biotechnology Advances **2010**, *28*, 142–150.

(49) Shalumon, K.T.; Anulekha, K.H; Chennazhi, K.P.; Tamura, H.; Nair, S.V.; Jayaku-mar, R. Fabrication of chitosan/poly (caprolactone) nanofibrous scaffold for bone and skin tissue engineering. *International Journal of Biological Macromolecules* **2011**, *48*, 571–576.

(50) Shalumon, K.T.; Sathish, D.; Chennazhi, K.P. ; Tamura, H. ; Nair,S.V.; Jayakumar, R. Fabrication of aligned poly (lactic acid)-chitosan nanofibers by novel parallel blade collector method for skin tissue engineering. *Journal of Biomedical Nanotechnology* **2012**, *8*, 405–416.

(51) Kose, R.;Kondo, T. Favorable 3-D-network formation of chitin nanofibers dispersed in water prepared using aqueous counter collision. *Sen-I Gakkaishi* **2011**, *67*, 91–95.

(52) Azuma, K.; Osaki, T.; Ifuku, S.; Saimoto, H.; Tsuka, T.; Imagawa,T.; Okamoto,Y.; Minami, S. α-Chitin nanofibers improve inflammatory and fibrosis responses in inflammatory bowel disease mice model .*Carbohydrate Polymers* **2012**, *90*, 197–200.

(53) Azuma, K.; Osaki, T.; Wakuda, T.; Ifuku, S.; Saimoto, H.; Tsuka, T.; Imagawa, T.; Okamoto, Y.; Minami, S. Beneficial and preventive effect of chitin nanofibers in a dextran sulfate sodium-induced acute ulcerative colitis model. *Carbohydrate Polymers* **2012**, *87*, 1399–1403.

(54) Ito, I.; Osaki, T.; Ifuku, S.; Saimoto, H.; Takamori, Y.; Kurozumi, S.; Imagawa, T.; Azuma, K.; Tsuka, T.; Okamoto, Y.; Minami, S. Evaluation of the effects of chitin nanofibers on skin function using skin models. *Carbohydrate Polymers* **2014**, *101*, 464–470.

(55) Ito, I.; Osaki, T.; Tokuda, K.; Asami, T.; Takamori, Y.; Kurozumi, S.; Ifuku, S.; Saimoto, H.; Imagawa, T.; Azuma, K.; Tsuka, T.; Okamoto, Y.; Minami, S. Effect of chitin nanofiber combined in rayon animal bedding on hairless mouse skin and on a three dimensional culture human skin model. *Journal of Chitin Chitosan Science* **2014**, *2*, 82–88.

(56) Dutta, A.K.; Kawamoto,N.; Sugino, G.; Izawa, H.; Morimoto, M.; Saimoto, H.; Ifuku, S. Simple preparation of chitosan nanofibers from dry chitosan powder by the star burst system. *Carbohydrate Polymers* **2013**, *97*, 363–367.

(57) Prashanth, K.V.P.; Kittur, F.S.; Tharanathan, R.N. Solid state structure of chitosan prepared under different N-deacetylating conditions. *Carbohydrate Polymers* **2002**, *50* 27–33.

(58) Wang, W.; Bo, S.; Li, S.; Qin, W. Determination of the Mark-Houwink equation for chitosans with different degrees of deacetylation. *International Journal of Biological Macromolecules* **1991**, *13*, 281–285.

(59) Ifuku, S.; Miwa, T.; Morimoto, M.; Saimoto, H. Preparation of highly chemoselective N-phthaloyl chitosan in aqueous media. *Green Chemistry* **2011**, *13*, 1499–1502.

(60) Fan, Y.; Saito, T.; Isogai, A. Preparation of chitin nanofibers from squid pen β-chitin by s imple mechanical treatment under acid conditions. *Biomacromolecules* **2008**b, *9*, 1919–1923.

(61) Fan, Y.; Fukuzumi, H.; Saito, T.; Isogai, A. Comparative characterization of aqueous dispersions and cast films of different chitin nanowhiskers/nanofibers. *International Journal of Biological Macromolecules* **2012**, *50*, 69–76.

(62) Lu, Y.; Sun, Q.; She, X.; Xia, Y.; Liu, Y.; Li, J.; Yang, D. Fabrication and characterization of α-chitin nanofibers and highly transparent chitin films by pulsed ultrasonication. *Carbohydrate Polymers* **2013**, *98*, 1497–1504.

(63) Mushi, N.E.; Butchosa, N.; Salajkova, M.; Zhou, Q.; Berglund, L. A. Nanostructured membranes based on native chitin nanofibers prepared by mild process. *Carbohydrate Polymers* **2014**, *112*, 255–263.

(64) Mushi, N. E.; Kochumalayil, J.; Cervin, N. T.; Zhou, Q.; Berglund, L. A. Nanostructurally controlled hydrogel based on small-diameter native chitin nanofibers: preparation, structure and properties. *ChemSusChem* **2016**, *9*, 989–995.

(65) Iwamoto, S.; Endo, T. 3 nm Thick lignocellulose nanofibers obtained from esterified wood with maleic anhydride. *ACS Macro Letters* **2015**, *4*, 80–83.

(66) Park, S.; Baker, J. O.; Himmel, M. E.; Parilla, P. A.; Johnson, D. K. Cellulose crystallinity index: measurement techniques and their impact on interpreting cellulase performance. *Biotechnology for Biofuels* **2010**, *3*, 1–10.

(67) Alexander, L. E. In A. R. Krieger (Ed.). X-ray diffraction methods in polymer science. *New York: Huntington* **1979.**

(68) Nogi, M.; Iwamoto, S.; Nakagaito, A. N.; Yano, H. Optically transparent nanofiber paper. *Advanced Materials* **2009**, *21*, 1595–1598.

(69) Tsutsumi, Y.; Koga, H.; Qi, Z.; Saito, T.; Isogai, A. Nanofiberlar chitin aerogels as renewable base catalysts. *Biomacromolecules* **2014**, *15*, 4314–4319.

(70) Ifuku, S.; Morooka, S.; Nakagaito, A.N.; Morimoto, M.; Saimoto, H. Preparation and characterization of optically transparent chitin nanofiber/ (meth) acrylic resin composites. *Green Chemistry* **2011**, *13*, 1708–1711.

(71) Ifuku, S.; Ikuta, A.; Egusa, M.; Kaminaka, H.; Izawa, H.; Morimoto, M.; Saimoto, H. Preparation of high strength transparent chitosan film reinforced with surface deacetylated chitin nanofibers. *Carbohydrate Polymers* **2013**, *98*, 1198–1202.

(72) Azuma, K.; Ifuku, S.; Osaki, T.; Okamoto, Y.; Minami, S. Preparation and biomedical applications of chitin and chitosan nanofibers. *Journal of Biomedical Nanotechnology* **2014**, *10*, 2891–2920.

(73) Azuma, K.; Izumi, R.; Kawata, M.; Nagae, T.; Osaki, T.; Murahata, Y.; Tsuka, T.; Imagawa, T.; Ito, N.; Okamoto, Y.; Morimoto, M; Izawa, H.; Saimoto, H.; Ifuku, S. Effects of oral administration of chitin nanofiber on plasma metabolites and gut microorganisms. *International Journal of Molecular Science* **2015**, *16*, 21931–21949.

(74) Izumi, R.; Komada, S.; Ochi, K.; Karasawa, L.; Osaki, T.; Murahata, Y.; Tsuka, T.; Imagawa, T.; Itoh, N.; Okamoto, Y.; Izawa, H. .;Morimoto, M.; Saimoto, H.; Azuma, K.; Ifuku, S. Favorable effects of superficially deacetylated chitin nanofibers on the wound healing process. *Carbohydrate Polymers* **2015**, *123*, 461–467.

(75) Izumi, R.; Azuma, K.; Izawa, H.; Morimoto, M.; Nagashima, M.; Osaki, T.; Tsuka, T.; Imagawa, T.; Ito, N.; Okamoto, Y.; H.; Saimoto, H.; Ifuku, S. Chitin nanofibers suppress skin inflammation in atopic dermatitis-like skin lesions in NC/Nga mice. *Carbohydrate Polymers* **2016**, *146*, 320–327.

(76) Ifuku, S.; Urakami, T.; Izawa, H.; Morimoto, M.; Saimoto, H. Preparation of a protein-chitin nanofiber complex from crab shells and its application as a reinforcement filler or substrate for biomineralization. *RSC Advances* **2015**, *5*, 64196–64201.

(77) Shimahara, K.; Takiguchi, Y. Methods in Enzymology. *Academic Press: Cambridge, MA, USA* **1998**, *161*, 417–423.

(78) Wei, H.; Shena, Q.; Zhao, Y.; Wang, D.J.; Xu, D.F. Influence of polyvinylpyrrolidone on the precipitation of calcium carbonate and on the transformation of vaterite to calcite. *Journal of Crystal Growth* **2003**, *250*, 516–524

(79) Fan, Y.; Saito, T.; Isogai, A. Individual chitin nano-whiskers prepared from partially deacetylated α-chitin by fibril surface cationization. *Carbohydrate Polymers* **2010**, *79*, 1046–1051.

(80) Xiong, D.; Chen, J.; Yu, T.; Gao, W.; Ling, X.; Li, Y.; Peng, S.; Huang, J. SPAD-based leaf nitrogen estimation is impacted by environmental factors and crop leaf characteristics. *Scientific Report* **2015**, *5*, 1–12.

List of publications

1. Aklog,Y.F.; Nagae,T. ; Izawa,H.;Morimoto,M.; Saimoto,H.; Ifuku,S. Effect of grinder pretreatment for easy disintegration of chitin into nanofiber. *Journal of Nanoscience and Nanotechnology* (in press). **[**Chapter 1**]**

2. Aklog,Y.F.; Dutta, A.K. ; Izawa,H.;Morimoto,M.; Saimoto,H.; Ifuku,S. Preparation of chitosan nanofibers from completely deacetylated chitosan powder by a downsizing process. *International Journal of Biological Macromolecules* **2015**, *72*, 1191–1195. **[**Chapter 2**]**

3. Aklog, Y .F.; Nagae, T. ; Izawa, H.; Morimoto, M.; Saimoto, H.; Ifuku, S. Preparation of chitin nanofibers by surface esterification of chitin with maleic anhydride and mechanical treatment. *Carbohydrate Polymers* **2016**, *153*, 55–59. **[**Chapter 3**]**

4. Aklog, Y .F.; Egusa, M.; Kaminaka, H.; Izawa, H.; Morimoto, M.; Saimoto, H.; Ifuku, S. Protein/$CaCO_3$/chitin nanofiber complex prepared from crab shells by simple mechanical treatment and its effect on plant growth. *International Journal of Molecular Science* **2016**, *17*, 1600. **[**Chapter 4**]**

Acknowledgements

Any significant milestone in one's life is made possible by the contributions of many people along the way. I would therefore like to offer my sincere thanks to all of them.

I would like to express my special appreciation and thanks to my honorable supervisor, Prof. Hiroyuki Saimoto, Department of Chemistry and Biotechnology, Graduate School of Engineering, for his helpful guidance and encouragement during the entire studies at Tottori University, Japan.

My special thanks goes to Dr. Shinsuke Ifuku, Associate Professor, Department of Chemistry and Biotechnology, Graduate School of Engineering, for his excellent advices, suggestions and continuous motivations from the beginning to the end of my study. As a beginner researcher, my work would have not been reached this level without his tremendous support.

I would like to thank Dr. Hironori Izawa, Assistant Professor Department of Chemistry and Biotechnology, Graduate School of Engineering, for his valuable guidance and encouragement. I am very grateful to all members of Saimoto Laboratory, for their continuous assistance during the research.

My deepest appreciation goes to my elder brother Dr. Dagnachew Aklog, Associate Professor, Center for International Affairs, for his initiation and motivation. His wife Hana Mesfin and their kids made my life enjoyable here in Tottori, which helped me to focus on my study.

I have special gratitude to my father Mr. Aklog Yihun, and my mother Ms. Tirualem Birhanu, for nursing me with affection and love and for dedicated partnership in the success of my life. I also wish to thank all my sisters, brothers, relatives and friends for supporting me spiritually throughout my study and my life in general.

I would like to thank my beloved wife Kidane Mihret and my son Ermyas Fantahun. Frankly speaking without their love, patience, and great sacrifice this work would not have been completed.

Last but not least, the author is much indebted to the Government of Japan, Ministry of Education, Culture, Sports, Science and Technology (MEXT) for the complete financial support for the last three and half years.